

**UNCLASSIFIED**

**AD NUMBER**

**ADB098392**

**LIMITATION CHANGES**

**TO:**

**Approved for public release; distribution is unlimited.**

**FROM:**

**Distribution authorized to U.S. Gov't. agencies and their contractors; Critical Technology; JAN 1986. Other requests shall be referred to Arnold Engineering Development Center, Attn: DOS, Arnold AFS, TN 37389-5000. This document contains export-controlled technical data.**

**AUTHORITY**

**AEDC/DO ltr, 20 Apr 1994**

**THIS PAGE IS UNCLASSIFIED**

AEDC-TR-85-65

copy 10

JUL 15 1992  
NOV 11 1992  
REF ID: A6222



## Spray Nozzle Calibrations

J. D. Hunt  
Sverdrup Technology, Inc.

January 1986

Final Report for Period October 1, 1981 – September 30, 1984

Distribution limited to U. S. Government agencies and their contractors; critical technology; January 1986. Other requests for this document shall be referred to Arnold Engineering Development Center/DOS, Arnold Air Force Station, TN 37389-5000.

**INFORMATION SUBJECT TO EXPORT CONTROL LAWS**  
This document may contain information subject to the International Traffic in Arms Regulation (ITAR) or the Export Administration Regulation (EAR) of 1979 which may not be exported, released or disclosed to foreign nationals inside or outside the United States without first obtaining an export license. A violation of the ITAR or EAR may be subject to a penalty of up to 10 years imprisonment and a fine of \$100,000 under 22 U.S.C. 2778 or Section 2410 of the Export Administration Act of 1979. Include this notice with any reproduced portion of this document.

PROPERTY OF U.S. AIR FORCE  
AEDC TECHNICAL LIBRARY

**TECHNICAL REPORTS  
FILE COPY**

ARNOLD ENGINEERING DEVELOPMENT CENTER  
ARNOLD AIR FORCE STATION, TENNESSEE  
AIR FORCE SYSTEMS COMMAND  
UNITED STATES AIR FORCE

## NOTICES

When U. S. Government drawings, specifications, or other data are used for any purpose other than a definitely related Government procurement operation, the Government thereby incurs no responsibility nor any obligation whatsoever, and the fact that the government may have formulated, furnished, or in any way supplied the said drawings, specifications, or other data, is not to be regarded by implication or otherwise, or in any manner licensing the holder or any other person or corporation, or conveying any rights or permission to manufacture, use, or sell any patented invention that may in any way be related thereto.

Qualified users may obtain copies of this report from the Defense Technical Information Center.

References to named commercial products in this report are not to be considered in any sense as an endorsement of the product by the United States Air Force or the Government.

## APPROVAL STATEMENT

This report has been reviewed and approved.

*David A. Duesterhaus*

DAVID A. DUESTERHAUS  
Directorate of Technology  
Deputy for Operations

Approved for publication:

FOR THE COMMANDER

*Lowell C. Keel*

LOWELL C. KEEL, Lt Colonel, USAF  
Director of Technology  
Deputy for Operations

**UNCLASSIFIED**

SECURITY CLASSIFICATION OF THIS PAGE

REPORT DOCUMENTATION PAGE				
1a. REPORT SECURITY CLASSIFICATION <b>Unclassified</b>		1b. RESTRICTIVE MARKINGS		
2a. SECURITY CLASSIFICATION AUTHORITY		3. DISTRIBUTION/AVAILABILITY OF REPORT Distribution limited to U.S. Government agencies and their contractors; critical technology; January 1986. Other requests for this		
2b. DECLASSIFICATION/DOWNGRADING SCHEDULE				
4. PERFORMING ORGANIZATION REPORT NUMBER(S) <b>AEDC-TR-85-65</b>		5. MONITORING ORGANIZATION REPORT NUMBER(S)		
6a. NAME OF PERFORMING ORGANIZATION <b>Arnold Engineering Development Center</b>		6b. OFFICE SYMBOL <i>(If applicable)</i> <b>DOP</b>	7a. NAME OF MONITORING ORGANIZATION	
6c. ADDRESS (City, State and ZIP Code) <b>Air Force Systems Command Arnold Air Force Station, TN 37389-5000</b>		7b. ADDRESS (City, State and ZIP Code)		
8a. NAME OF FUNDING/SPONSORING ORGANIZATION <b>Arnold Engineering Development Center</b>		8b. OFFICE SYMBOL <i>(If applicable)</i> <b>DOT</b>	9. PROCUREMENT INSTRUMENT IDENTIFICATION NUMBER	
8c. ADDRESS (City, State and ZIP Code) <b>Air Force Systems Command Arnold Air Force Station, TN 37389-5000</b>		10. SOURCE OF FUNDING NOS		
11. TITLE (Include Security Classification) <b>Spray Nozzle Calibrations</b>		PROGRAM ELEMENT NO. <b>921E06 65807F</b>	PROJECT NO. <b>D188EW</b>	TASK NO.
12. PERSONAL AUTHORIS <b>Hunt, Jay D., Sverdrup Technology, Inc., AEDC Group</b>		WORK UNIT NO.		
13a. TYPE OF REPORT <b>Final</b>	13b. TIME COVERED <b>FROM 10/1/81 To 9/30/84</b>		14. DATE OF REPORT (Yr., Mo., Day) <b>January 1986</b>	
15. PAGE COUNT <b>74</b>				
16. SUPPLEMENTARY NOTATION <b>Available in Defense Technical Information Center (DTIC).</b>				
17. COSATI CODES		18. SUBJECT TERMS (Continue on reverse if necessary and identify by block number)		
FIELD <b>13</b>	GROUP <b>07</b>	SUB. GR. <b></b>	spray nozzles icing clouds	calibration liquid water content
				mass median droplet diameter
19. ABSTRACT (Continue on reverse if necessary and identify by block number) <p>Spray nozzle calibration techniques were evaluated. Ten spray nozzles to be utilized for producing simulated icing clouds were calibrated to determine the ranges of mass median droplet diameter and water flow rate. The number and types of spray nozzles calibrated were: (1) two internal mixing, (2) five external mixing, and (3) three sonic mixing nozzles. The calibration results are presented. A comparison was made of the calibration from NASA Lewis Research Center's (NASA-LeRC) Icing Research Tunnel (IRT) and the calibration at AEDC of a NASA-LeRC Standard spray nozzle produced as part of this study. Based upon the comparison, it was concluded that the calibration of a single spray nozzle can be utilized as the calibration of a multinozzle spray bar configuration. From a study of the effects of cell airspeed on the nozzle calibration, it was concluded that no airspeed dependency exists for the calibration. The theoretical liquid water content distribution (LWC) was calculated for a natural icing cloud, and the results were compared with the LWC results obtained as part of this study. It was found that the 10 spray nozzles did</p>				
20. DISTRIBUTION/AVAILABILITY OF ABSTRACT <input type="checkbox"/> UNCLASSIFIED/UNLIMITED <input checked="" type="checkbox"/> SAME AS RPT. <input checked="" type="checkbox"/> DTIC USERS <input type="checkbox"/>		21. ABSTRACT SECURITY CLASSIFICATION <b>Unclassified</b>		
22a. NAME OF RESPONSIBLE INDIVIDUAL <b>W.O. Cole</b>		22b. TELEPHONE NUMBER <i>(Include Area Code)</i> <b>(615) 454-7813</b>	22c. OFFICE SYMBOL <b>DOS</b>	

UNCLASSIFIED

SECURITY CLASSIFICATION OF THIS PAGE

3. DISTRIBUTION/AVAILABILITY OF REPORT. Concluded.

document shall be referred to Arnold Engineering Development Center/DOS, Arnold Air Force Station, TN 37389-5000.

19. ABSTRACT. Concluded.

not produce comparable distributions at large mass median droplet diameters. However, an analysis technique utilizing the distribution data obtained for the nozzles was recommended.

UNCLASSIFIED

SECURITY CLASSIFICATION OF THIS PAGE

## PREFACE

The work reported herein was conducted by the Arnold Engineering Development Center (AEDC), Air Force Systems Command (AFSC). The Air Force project manager was Mr. David A. Duesterhaus. The results were obtained by Sverdrup Technology, Inc., AEDC Group, operating contractor for the aeropropulsion testing effort at the AEDC, AFSC, Arnold Air Force Station, Tennessee, under Project No. D188EW. The work was performed during the period from October 1, 1981 to September 30, 1984. The manuscript was submitted for publication on October 2, 1985.

## CONTENTS

	<u>Page</u>
<b>1.0 INTRODUCTION</b>	
1.1 General .....	5
1.2 Background .....	6
1.3 Scope of Investigation .....	7
1.4 Outline of Report .....	7
<b>2.0 EXPERIMENTAL APPARATUS AND PROCEDURES</b>	
2.1 Icing Research Test Cell .....	7
2.2 Icing Instrumentation and Method .....	8
2.3 Spray Nozzles .....	9
2.4 Supporting Instrumentation .....	10
2.5 Test Procedures .....	11
2.6 Precision of Measurements .....	12
<b>3.0 RESULTS AND DISCUSSION</b>	
3.1 Introduction .....	12
3.2 Calibration Results .....	12
3.3 Comparison of Calibrations .....	18
3.4 Effect of Velocity .....	19
3.5 Natural Icing Cloud Comparisons .....	20
<b>4.0 CONCLUSIONS AND RECOMMENDATIONS</b>	21
<b>REFERENCES</b> .....	22

## ILLUSTRATIONS

<u>Figure</u>	<u>Page</u>
1. Cloud Icing Condition .....	25
2. Icing Research Test Cell .....	27
3. Fiber-Optics Particle-Sizing System .....	30
4. FOS Optical Arrangement .....	31
5. Spray Nozzles .....	32
6. Droplet Size Calibration, SS $\frac{1}{4}$ J-26B Nozzle .....	35
7. Water Flow Calibration, SS $\frac{1}{4}$ J-26B Nozzle .....	36
8. Droplet Size Calibration, SS $\frac{1}{4}$ J-2050 Nozzle .....	37
9. Water Flow Calibration, SS $\frac{1}{4}$ J-2050 Nozzle .....	38
10. Droplet Size Calibration, NASA LeRC Standard Nozzle .....	39
11. Water Flow Calibration, NASA LeRC Standard Nozzle .....	40

<u>Figure</u>	<u>Page</u>
12. Droplet Size Calibration, NASA LeRC Model I Nozzle .....	41
13. Water Flow Calibration, NASA-LeRC Model I Nozzle .....	42
14. Droplet Size Calibration, NASA-LeRC Model II Nozzle .....	43
15. Water Flow Calibration, NASA-LeRC Model II Nozzle .....	44
16. Droplet Size Calibration, SS $\frac{1}{4}$ J-1A Nozzle .....	45
17. Water Flow Calibration, SS $\frac{1}{4}$ J-1A Nozzle .....	46
18. Droplet Size Calibration, SS $\frac{1}{4}$ J-1 Nozzle .....	47
19. Water Flow Calibration, SS $\frac{1}{4}$ J-1 Nozzle .....	48
20. Droplet Size Calibration, Sonicore #125 Nozzle .....	49
21. Water Flow Calibration, Sonicore #125 Nozzle .....	50
22. Droplet Size Calibration, Sonicore #052 Nozzle .....	51
23. Water Flow Calibration, Sonicore #052 Nozzle .....	52
24. Droplet Size Calibration, Sonicore #035 Nozzle .....	53
25. Water Flow Calibration, Sonicore #035 Nozzle .....	54
26. Scatter Diagram AEDC versus NASA-LeRC Calibrations of Standard NASA Nozzle .....	55
27. Effect of Cell Airspeed on Calibration .....	56
28. Drop Size Distribution in Nature for a Range of MMD at Same LWC .....	57
29. Droplet Size Distribution for Nozzles .....	58

## TABLES

1. Icing Research Cell Performance Capability .....	68
2. Parameter Measurement Uncertainty .....	69
 NOMENCLATURE .....	70

## 1.0 INTRODUCTION

### 1.1 GENERAL

The formation of ice on aircraft surfaces occurs during flight through clouds of supercooled water droplets. Ice accretion on these surfaces usually results in a degradation of both aircraft performance and operational safety. Therefore, protective devices for removing accumulated ice (deicing devices) or for continuously maintaining the exposed surfaces of the aircraft free of ice (anti-icing devices) are routinely used. For safety reasons, the effectiveness of the protective devices must be determined before their use; hence, each device must be tested under simulated atmospheric icing conditions.

The meteorological conditions to be simulated during testing have been characterized and documented in the "Airworthiness Standards," Ref. 1. The ranges of temperature, liquid water content, and droplet size at various altitudes from stratiform (layer) and cumuliform clouds are shown as envelopes in Fig. 1. These envelopes define the maximum likely ranges of the parameters that would occur in nature (that is, 99.9 percent of the icing observations in nature are within the envelopes). Every combination of the parameters represented by the envelopes, along with the mission scenario of the aircraft, is utilized to determine the specific conditions that result in the most severe icing conditions for each aircraft component. The discrete conditions become the design and test conditions for icing testing of the aircraft, its components, and icing protection systems. It is important, therefore, that an icing simulation facility operate over as large a portion of the icing envelope as possible.

Icing conditions are simulated by duplicating the principal factors that characterize an icing cloud: (1) air temperature, (2) droplet size distribution (including the "mean effective" droplet diameter for the droplet size distribution), and (3) cloud liquid water content (LWC). During icing testing, a cloud is simulated by injecting a continuous spray of water droplets into a cold airstream directed at aircraft components to be tested. The water spray is injected by a bank of pneumatic spray nozzles located upstream of the test article, usually in the low-velocity region of the test cell or wind tunnel. Both the LWC and mean effective droplet size are set and maintained through variations in the water and air supply pressures of the spray nozzles.

Establishment and control of a simulated icing cloud requires knowledge of the LWC and mean effective droplet diameter produced by a spray nozzle system as a function of the spray nozzle inlet air and water pressures. For this reason, spray nozzle systems are calibrated before testing.

The frequency and method of calibrating a spray nozzle system varies from facility to facility. For example, the nozzles of the Icing Research Tunnel (IRT) located at NASA Lewis Research Center (NASA-LeRC) were calibrated utilizing rotating multicylinders and oil slides. The calibration of the IRT has changed very little over a 20-year period (Ref. 2). Therefore, recalibration of the spray system has not been required. The stability of the IRT calibration has been realized because the spray nozzle type, number, and locations are not routinely changed. On the other hand, none of the engine test cells at the Arnold Engineering Development Center (AEDC) Engine Test Facility (ETF) are dedicated solely for the purpose of icing testing. The types of spray nozzles, as well as their number and location, change from test to test. Therefore, there exists at the AEDC/ETF a potential requirement for large numbers of in-cell spray nozzle calibrations.

## 1.2 BACKGROUND

Because of concerns over the effectiveness of producing a specified icing environment in the test cell at AEDC, an icing technology program was initiated. As part of the technology program, efforts have been made to improve the spray nozzle calibration capabilities. To date, these efforts have centered around improving measurement techniques for defining the droplet size distribution (Ref. 3). These initial efforts resulted in selection of a near-real time droplet sizing technique (Ref. 3). However, because of the logistics of installing and removing the droplet sizer for each icing cloud calibration, application of the technique to in-cell calibrations would be costly and time consuming. Thus, the required large number of in-cell calibrations is prohibitive from an economic and scheduling standpoint.

The AEDC icing technology program was expanded to include an in-depth evaluation of spray nozzle calibration techniques. Also, as part of the expanded icing program, a Memorandum of Understanding (MOU) between the AEDC and NASA-LeRC was issued to provide for data and hardware exchanges between the two agencies. The MOU was utilized by the two agencies to exchange spray nozzles and the calibration data obtained from the spray nozzles, thereby providing a foundation for the in-depth evaluation of spray nozzle calibration techniques.

In addition to the spray nozzle calibration study, the icing capabilities of the AEDC/ETF engine test cells were to be expanded to encompass a larger portion of the FAR-25 icing envelope as defined by Fig. 1; this, too, was part of the expanded AEDC icing technology program. Since both the AEDC and NASA-LeRC desired to expand their icing testing capabilities to include the proposed icing envelope expansion, this portion of the AEDC icing technology program was also included in the MOU.

### **1.3 SCOPE OF INVESTIGATION**

A research program was conducted at the AEDC/ETF to evaluate and refine the spray nozzle calibration techniques. The objectives of the study were (1) to reduce the required number and frequency of spray nozzle calibrations during icing testing of engines; and (2) to expand the icing testing capabilities of the AEDC/ETF to include a larger portion of the FAR-25 icing envelope.

To achieve the program objectives required (1) review of the spray nozzle calibrations and calibration techniques of other agencies; (2) calibration of the spray nozzles of other agencies in the AEDC Icing Research Facility; and (3) analysis and comparison of the AEDC data to the calibration data of other agencies.

### **1.4 OUTLINE OF REPORT**

This report documents the findings of the evaluation of the spray nozzle calibrations. Section 2.0 is a description of the experimental apparatus and procedures utilized. The research test cell is described, and its operating characteristics are summarized, and descriptions of the instrumentation systems and the measurement uncertainties are presented.

The results and analysis of the results are given in Section 3.0. The analysis includes information obtained from other agencies, the calibrations obtained at the AEDC, velocity effects on calibration data, and comparisons of calibrations between facilities, as well as with natural cloud conditions.

Conclusions and recommendation are presented in Section 4.0.

## **2.0 EXPERIMENTAL APPARATUS AND PROCEDURES**

### **2.1 ICING RESEARCH TEST CELL**

A research test cell has been developed for the sole purpose of studying icing environments. The research cell, a subscale version of the AEDC propulsion development test cells, can provide the meteorological icing condition described in Fig. 1 for airflows up to 30 lbm/sec. Table 1 summarizes the research test cell characteristics pertinent to the icing experiments.

The icing research test cell (Figs. 2a and b) consists of a flowmetering venturi, plenum chamber, water spray system, bellmouth, removable inlet connecting ducts, and a test chamber. A secondary air supply system also provides air to the test chamber; this secondary air encapsulates the primary air to prevent recirculation of the icing cloud water droplets through the measurement plane (Fig. 2a).

The plenum chamber rides on casters along rails. It can be moved in the axial direction; hence, the axial distance between the spray nozzle (located in the plenum chamber) and the test section can be varied without moving the test chamber. This makes it possible to study water droplet formation as a function of axial position without relocating the particle diagnostics instrumentation.

The water spray system, which provides filtered, demineralized water and atomizing air to the spray nozzle, is shown in Fig. 2c. A single water spray nozzle provides the droplet cloud. This spray nozzle is located on the centerline of the plenum chamber and is attached to a movable screw assembly. The axial position of the spray nozzle can be varied from 12 to 16 in. upstream of the bellmouth.

The test chamber (Figs. 2a and b) has six instrumentation and/or viewing ports around its circumference. The icing cloud, which issues from the connecting duct into the test chamber as a free jet, can be viewed through all of the ports. The test plane--the plane along which all droplet size measurements are made--coincides with the centerline of the ports.

## 2.2 ICING INSTRUMENTATION AND METHODS

### 2.2.1 Droplet Sizing System

The droplet size distribution of each icing cloud was measured using a fiber-optics sizing system (FOS). The FOS is an imaging device that uses an expanded laser beam (as a light source) and an optical system to define a probe volume in the particle flow field (Fig. 3). The probe volume is focused onto a linear array of sensor modules. As a particle passes through the probe volume, its shadow occludes a number of the sensors. The number of sensor modules occluded is proportional to the particle diameter. Reference 4 gives a more detailed discussion of the theory and application of the FOS.

The FOS used in the icing research test cell is shown schematically in Fig. 4. The illumination for the probe volume, located on the test cell centerline, is provided by an air-cooled 25-mw argon laser. The laser beam is spatially filtered and focused by a Spectra-Physics® collimator and directed by a front surface mirror through a test cell window.

The light-collecting optics of the FOS, in conjunction with a cross-beam coincidence system, define the optical probe volume. Both the collecting optics and the coincidence system are located outside the test cell opposite the argon laser (Fig. 4). The light-collecting optics are aligned along the laser axis, and the cross-beam coincidence system is inclined to the laser axis by 12.83 deg. The probe volume is magnified 83 times and projected by the collecting optics onto an array of 32 optical fibers or "light pipes." The coincidence system is used to define the probe volume and to eliminate the spurious effects of noise coupled with out-of-focus particle transits. The individual optical fibers, which are 264  $\mu\text{m}$  in diameter, are arrayed along a straight line for a total length of 0.3325 in.; each fiber terminates at a photomultiplier (PM) tube. Each of the 32 photodetector circuits provides information to the size-determination logic of the data handling system, as described in Ref. 4. The number of events of specified size is stored and displayed periodically on both a cathode ray tube (CRT) and a digital display on the front panel of the particle data system.

Thirty channels of droplet size data are stored by the data handling system of the FOS. Data are output from the FOS data handling system to a Tektronix® 4051 minicomputer; data output is controlled from the minicomputer keyboard. The channel number and the droplet counts corresponding to that channel comprise the data input to the minicomputer. The data are reduced by the minicomputer to the desired form, and hard copies of the reduced data are provided online. Measures of the mass median droplet diameter (MMD), as well as other statistical quantities, are provided in near-real time, that is, within 2 min of data acquisition.

### 2.2.2 Liquid Water Content (LWC)

The LWC, unlike the droplet size distribution, is not measured online, but is calculated from measurements of the cell primary airflow and spray nozzle water flow rate. The water flow rate into the cell is the sum of the liquid water at the test section and the amount of spray water evaporated during the time it takes the droplets to travel from the injection point to the test section. The amount of water evaporated is analytically determined from a mathematical model developed at the AEDC (Ref. 5). Thus, by precisely measuring the primary airflow and injected water flow rates, the liquid water content was accurately determined. For a validation of the technique, see Ref. 6.

## 2.3 SPRAY NOZZLES

The only type of spray nozzle that can produce a droplet cloud with the required droplet size distribution and the necessary concentrations is a two-fluid atomizer (Ref. 7). Therefore, only this type of spray nozzle was investigated during this study.

Further, three classes of two-fluid atomizers were studied: (1) internal mixing, (2) external mixing, and (3) sonic mixing. Each class will be discussed.

### **2.3.1 Internal Mixing**

A cross-sectional schematic of an internal mixing spray nozzle is shown in Fig. 5a. The water and airstreams come together and are mixed within the air cap, and atomization is provided as the mixture is forced through the holes of the air cap.

Two geometrically similar spray nozzles of this class were calibrated. The basic dimension of each is shown in Fig. 5a.

### **2.3.2 External Mixing**

Atomization is accomplished by impingement of the high-velocity atomizing airstream with the water stream for the external mixing spray nozzle. Impingements occur just as the two streams exit the nozzle. Cross-sectional schematics of two external mixing nozzles are shown in Fig. 5b.

Five spray nozzles of this class were calibrated. The different geometries, designations, and basic dimensions are provided in Fig. 5b.

### **2.3.3 Sonic Mixing**

Atomization is accomplished by the sonic mixing nozzle in two steps. The water streams impinge with the airstream just inside the exit of the nozzle. The resulting water spray is further atomized by interaction with a shock wave caused by the impinging atomizing airstream with the resonator chamber downstream of the nozzle exit.

Three geometrically similar sonic mixing spray nozzles were calibrated. The basic dimensions of the nozzles are shown in Fig. 5c.

## **2.4 SUPPORTING INSTRUMENTATION**

Conventional instrumentation was required to determine test conditions during the experimental program. The instrumentation stations are indicated in Fig. 2a. Total temperatures were measured with single-shielded, self-aspirating, copper-constantan thermocouple probes with an ambient reference junction. Pressures were measured with strain-gage-type absolute pressure transducers referenced to atmospheric pressure.

Two turbine-type flowmeters, installed in parallel in the water line to the spray nozzle, were used to determine the water content of the icing cloud. One flowmeter had a dynamic range of 2.4 to 6.0 gph and was used to measure the larger water flow rates, while the smaller water flow rates were measured utilizing the second flowmeter, the dynamic range of which was 0.6 to 3.0 gph. The flowmeters measured all water flowing into the test cell through the spray nozzle and provided primary water content data.

Two hot-wire-type flowmeters were utilized for measuring mass flow of the atomizing air through the spray nozzle. As in the case of the water flowmeters, the airflow meters were installed in parallel in the atomizing air line. One flowmeter was used to measure the larger atomizing air flow rates with a dynamic range of 5 to 15 standard cubic feet per minute (SCFM) while the second flowmeter was utilized to measure the smaller flow rates, with a dynamic range of 1.5 to 5 SCFM.

## 2.5 TEST PROCEDURES

All instrumentation parameters of the support instruments were calibrated before each test. The calibrations were conducted in place with ambient pressure in the test cell. The calibrations included millivolt calibration of all temperature parameters and resistance calibration of all pressure parameters. All calibrations were reviewed and discrepancies were corrected before the test.

After calibrations were performed, the test cell pressure was reduced to the desired pressure altitude. Cell conditions were allowed to stabilize for approximately 5 min, and a data point was obtained for final instrumentation check. During cell stabilization, a final alignment check was made on the FOS.

After the final instrumentation check, both primary and secondary inlet air was admitted to the test cell at the required pressure and temperature. Airflow through the spray nozzle was also started and maintained throughout the test to prevent freezing of the spray nozzles. Once the test cell flow conditions had stabilized, the air purge through the water outlet of the spray nozzle was stopped, and the desired spray water and atomizing air pressures were set for the spray nozzle. Droplet size information was then obtained utilizing the FOS; at least three droplet size histograms were taken for each spray nozzle test condition. A minicomputer was used to record the test cell data acquired concurrently with the FOS data. When this test sequence was complete, the next spray nozzle condition was established by holding the atomizing air pressure constant and changing the spray water pressure; the data acquisition process was then repeated.

The test matrix consisted of the aerodynamic test conditions and the spray nozzle test conditions. For this effort, all testing was accomplished at the same aerodynamic conditions; the primary inlet air was maintained at a bulk velocity ( $V_\infty$ ) of 220 fps, with a total temperature ( $T_0$ ) of 10° F and a cell static pressure ( $P_\infty$ ) of 13.7 psia. Each nozzle was calibrated over a range of atomizing air and water pressures. This range of pressures described the spray nozzle test conditions. Although the attainable range differed from nozzle to nozzle, the calibrations were confined to air pressure above the critical limit (approximately 26 psia for these tests). Both the spray water and atomizing air were heated before injection to eliminate freezing of the droplets because of expansion through the spray nozzle. The air and water temperature used were 200° F and 180° F, respectively.

This test procedure was utilized throughout the program. The FOS was utilized to determine the water droplet distribution for each spray nozzle over the range of attainable inlet pressures for the nozzle. From the droplet size distribution a measure of the central tendency was obtained (for all calibrations the MMD was used) and along with the water pressure and atomizing air pressure, constituted a calibration point.

## 2.6 PRECISION OF MEASUREMENTS

Uncertainties (bands which include 95 percent of the calibration data) of the basic experimental parameters were estimated from repeat calibrations of the instrumentation systems. These uncertainties were estimated against secondary standards whose precisions are traceable to the NBS. The uncertainties were combined by means of the Taylor series method of error propagation (Ref. 8) to determine the precision of the experimental parameters presented in Table 2.

## 3.0 RESULTS AND DISCUSSION

### 3.1 INTRODUCTION

Since the objectives of the study were to extend the AEDC's icing testing capabilities and to reduce the number and frequency of nozzle calibrations, it was necessary to study different types of spray nozzles. On the one hand, nozzles interchangeable with the spray nozzles presently used at the AEDC were to be studied. This would eliminate modification to the AEDC spray system (provided the nozzles did, indeed, provide the desired increase in capability). On the other hand, nozzles with a known calibration were required to provide the needed data base for comparison when the calibration techniques were studied.

The present AEDC spray system was built to accommodate the Spraying System Company's  $\frac{1}{4}$ J series nozzles (Ref. 9). Therefore, four Spraying Systems nozzles were

selected for calibration. Complete calibration did not exist for the nozzles selected. A complete calibration did exist, however, for the NASA-LeRC external mixing spray nozzles (Ref. 10). The nozzles are installed in the Icing Research Tunnel (IRT), and were calibrated in the late 1940's and early 1950's. Rotating multicylinders and oil slides were used to calibrate the IRT nozzle system. Because of the existence and accessibility of the calibration, the NASA-LeRC nozzles were selected for further study.

Two other NASA-LeRC external mixing nozzles were also selected for study. Both are identical to the original (Standard) NASA nozzle, except the water tube diameter of each has been reduced (Fig. 5b). Calibration of these nozzles was accomplished to aid NASA-LeRC in selection of a nozzle design that would extend the operational envelope of the IRT.

Three sonic mixing nozzles manufactured by the Sonic Development Company were also selected for calibration. A partial calibration exists for one of the spray nozzles (Sonicore #125), but it has not been published. [The Sonicore #125 has been selected for use on the U.S. Army's Helicopter Icing Spray System (HISS)]. The other two Sonicore® nozzles were selected to evaluate a possible extension to operating envelopes of systems utilizing the Sonicore nozzles.

In this section of the report, the results of the study and an analysis of the results are presented. The calibration results are followed by a comparison of calibration results to those of NASA-LeRC. The effects of the airstream velocity on droplet size are then presented. Section 3.5 contains a comparison of the calibration results with natural cloud data.

## 3.2 CALIBRATION RESULTS

### 3.2.1 Internal Mixing Nozzles

The results obtained on the two internal mixing spray nozzles are illustrated in Figs. 6-9. Figures 6 and 8 show plots of MMD as a function of the nozzle mass flow ratio. (The mass flow ratio is defined as the mass flow rate of spray nozzle atomizing air divided by the mass flow rate of spray water.) The water flow rates for various water pressures, atomizing air pressures, and mass flow ratios are presented in Figs. 7 and 9. Thus, Figs. 6 and 7 comprise a calibration for SS ¼J-26B, and Figs. 8 and 9 are the calibration for SS ¼J-2050.

A power curve of the form  $y = ax^k$  was fitted to the droplet size calibration data and is shown as the solid line in Figs. 6 and 8. The regression coefficients for the curve fits were determined by the least-squares method. The curve-fit equations for the SS ¼J-26B and SS ¼J-2050 are, respectively,

$$\overline{D_m} = 17.97 \left( \frac{\dot{W}_a}{\dot{W}_w} \right)^{-0.318},$$

and

$$\overline{D_m} = 18.84 \left( \frac{\dot{W}_a}{\dot{W}_w} \right)^{-0.338}.$$

The dashed lines shown in Figs. 6 and 8 serve to illustrate that 95 percent of the calibration data fall within  $\pm 5 \mu\text{m}$  of the curves.

The droplet diameter calibration for both nozzles, Figs. 6 and 8, is seen to be fairly "flat" in the 15- to 25- $\mu\text{m}$  range; large changes in the mass flow ratio are required to produce small changes in the mass median diameter. In this range, the mass flow ratio can be used with a high level of confidence to determine the MMD of the icing cloud. That the MMD characteristics of both the SS- $\frac{1}{4}\text{J}-26\text{B}$  and SS  $\frac{1}{4}\text{J}-2050$  are so similar is not surprising, since identical air caps are used to form the droplet spray (Fig. 5a).

The principal differences between the SS  $\frac{1}{4}\text{J}-26\text{B}$  and SS  $\frac{1}{4}\text{J}-2050$  can be found in the water flow calibration of the nozzles, Figs. 7 and 9. From Fig. 7, the flow rate range provided by the SS  $\frac{1}{4}\text{J}-26\text{B}$  is shown to be 0.04 to 0.25 gpm, while the range for the SS  $\frac{1}{4}\text{J}-2050$  is seen to be smaller, 0.015 to 0.06 gpm (Fig. 9).

The water flow calibration also serves to illustrate the interdependencies of the air and water pressure. A change in the air pressure will result in a corresponding change in water pressure, and vice versa. When changing from one condition (water flow and/or MMD) to another, the air and water pressure must be alternately changed to iterate onto the new set point. This characteristic is indicative of internal mixing spray nozzles, and for this reason, these nozzles are difficult to use for icing testing unless an automatic pressure control for both pressures is used.

With the spray system described in Section 2.0, the maximum water and air pressures attainable for the two interval mixing nozzles were 200 psia (Figs. 8 and 9). For this range of pressures, the calibration data reveal that the SS  $\frac{1}{4}\text{J}-26\text{B}$  and SS  $\frac{1}{4}\text{J}-2050$  can be utilized as spray nozzles to produce an icing cloud with MMD's in the range of 15 to 25  $\mu\text{m}$  and water flow rates of 0.015 to 0.25 gpm.

The AEDC utilizes both the SS  $\frac{1}{4}\text{J}-26\text{B}$  and the SS  $\frac{1}{4}\text{J}-2050$  to produce clouds during icing testing (Ref. 3). The icing systems that provide the water and atomizing air during the tests have capabilities similar to those of the icing research cell. Therefore, the range of

MMD's and water flow rates produced in the AEDC test cells is limited to the values defined above. Since one of the objectives of the icing technology program was to extend the icing testing capabilities of the AEDC to cover a larger portion of the FAR-25 icing envelope, other types of nozzles were examined and calibrated.

### 3.2.2 External Mixing

The calibration data obtained for the five external mixing nozzles are shown in Figs. 10-19. A calibration consists of two figures: one describes the MMD as a function of the nozzle correlating parameter, and the second illustrates the water flow rate as a function of the atomizing air and water pressures.

Figures 10 and 11 comprise the calibration for the standard NASA-LeRC spray nozzle. As seen in Fig. 10, the range of MMD's for the standard nozzle is from 12.4 to 38.3  $\mu\text{m}$ ; the correlating parameter,  $\Delta P$ , is defined as the differences between the spray water pressure and the atomizing air pressures. The water flow rate (Fig. 11) is seen to vary from 0.056 to 0.206 gpm for the same correlating parameter. Thus, for a spray system capable of providing the water and atomizing air pressures as defined in Table 1, the standard NASA-LeRC spray nozzle can provide an icing cloud with MMD's in the range of 12.4 to 38.3  $\mu\text{m}$ , with water flow rates of 0.05 to 0.206 gpm.

NASA-LeRC reduced the water tube diameter of the standard spray nozzle by 38 percent; the resulting spray nozzle is the Model I configuration of Fig. 5b. By reducing the water tube size, the water flow rate through the nozzle will be reduced (for the same water pressures), and if the range of droplet diameters is not substantially altered from those observed for the standard nozzle, the Model I nozzle could be utilized in place of the standard nozzle to produce lower liquid water content clouds. Figures 12 and 13, presenting the calibration for the Model I nozzle, substantiate the notion, for the MMD's are seen to vary from 9.5 to 32.6  $\mu\text{m}$ , approximately the same range achievable with the standard nozzle, while the water flow rate ranges from 0.025 to 0.10 gpm. Not only are the maximum and minimum flow rates attainable with Model I nozzle lower than those of the standard nozzle, but the range of flow rates is also smaller. The Model I spray nozzle can, therefore, be utilized as a substitute for the standard spray nozzle when a lower liquid water content is desired.

The third NASA-LeRC nozzle calibrated was the Model II configuration of Fig. 5b. The Model II nozzle contained a water tube that was reduced in diameter by 64 percent from the standard spray nozzle. Again, the reduction in tube diameter was intended to provide lower water flow rates with a range of MMD's comparable to those of the standard nozzle.

The calibration for the Model II nozzle, Figs. 14 and 15, illustrates that a reduction in the range of MMD's has occurred along with the reduction in water flow rate (Fig. 14); the principal range of MMD's is seen to exist for nozzle air pressures equal to or greater than 35 psia; the maximum value is 14.5  $\mu\text{m}$ , and the minimum is 9.0  $\mu\text{m}$ . The second range of MMD's occurs for a nozzle air pressure of 30 psia, and is seen to be from 19.3 to 21  $\mu\text{m}$ . Droplet size calibrations were not conducted for nozzle air pressures between 30 and 35 psia.

Examination of the data of Fig. 14 reveals that the water pressure has little effect on the MMD's. This suggests that the momentum of the atomizing airstream becomes overpowering for a critical air pressure somewhere in the range of 30 to 35 psia. Once the critical pressure is reached, the resulting MMD's become insensitive to water pressure. An increase in the water tube diameter or a decrease in the diameter of the air orifice would ensure a greater degree of influence on MMD's by water pressure; the desired amounts are not known and this aspect is beyond the scope of this program.

The water flow rates for the Model II nozzle are seen to vary from 0.014 to 0.028 gpm (Fig. 15). The goal of reducing the water flow rate was achieved with this nozzle, however, at the expense of not being able to control the MMD's over a range of droplet diameter equivalent to the standard nozzle. The Model II nozzle cannot, therefore, be utilized as a substitute for the standard spray nozzle.

Two external mixing nozzles manufactured by Spraying Systems Company were also calibrated. The results are shown in Figs. 16-19; the SS $\frac{1}{4}$ J-1A calibration is shown in Figs. 16 and 17, and Figs. 18 and 19 show the calibration for the SS $\frac{1}{4}$ J-1.

The MMD's performance as functions of water flow rate, the correlating parameters for both nozzles, is shown in Figs. 16 and 18. Both nozzles are seen to provide MMD in approximately the same size range, from 10 to 38  $\mu\text{m}$ . Also, it is seen that both nozzles have the same operating characteristics; that is, an increase in water pressure produces larger MMD's for a constant air pressure.

The water flow rate ranges, Figs. 17 and 19, however, are seen to be different with no overlap of the two ranges. The SS $\frac{1}{4}$ J-1A operates over a range of 0.0075 to 0.03 gpm, while the SS $\frac{1}{4}$ J-1 has an operating range of 0.058 to 0.120 gpm. As seen from the calibration, both spray nozzles produce icing clouds that are within the FAR-25 icing envelope. However, only the SS $\frac{1}{4}$ J-1A can produce clouds that extend the AEDC's present icing testing capabilities (see Figs. 6-9). Therefore, a complete calibration of the SS $\frac{1}{4}$ J-1A was conducted, while only a partial calibration of the SS $\frac{1}{4}$ J-1 was conducted.

### 3.2.3 Sonic Mixing Nozzles

Figures 20–25 illustrate the results obtained from the three Sonicore nozzles. Figures 20 and 21 are the calibration set for the Sonicore #125, Figs. 22 and 23 are for the Sonicore #052, and the Sonicore #035 results are presented in Figs. 24 and 25.

The MMD's as a function of water flow rate are shown in Figs. 20, 22, and 24. The Sonicore #125 is seen to produce MMD's in the 13.5 to 44  $\mu\text{m}$  range (Fig. 20) while the Sonicore #052 and #035 nozzles produce MMD's over identical ranges, 9.0 to 45  $\mu\text{m}$  (Figs. 22 and 24).

As seen from the water flow calibration for the Sonicore #125, (Fig. 21), the range of flow rates varies from 0.02 to 0.3 gpm. The range of flow rates is obtained for water pressures less than 40 psia. The calibration could not be extended with the present spray system because the upper limit of the water flow meters was reached.

The flow rate ranges for the Sonicore #052 and #035 are seen to be 0.075 to 0.26 gpm and 0.017 to 0.188 gpm, respectively (Figs. 23 and 25). It should be noted that for atomizing air pressure less than 110 psia, the calibrations are very steep, and small changes in water pressure will result in large changes in the water flow rate. If these nozzles are used as atomizers for producing icing clouds, very precise control of the water pressure will be required.

Either the Sonicore #052 or #035 can be utilized to produce MMD's and provide water flow rates which extend the operational envelope produced by the Sonicore #125. However, the Sonicore #035 is selected as the best choice for replacement of the #125 because the slopes of the water calibration curves are less steep than those of the #052, (see Figs. 23 and 25).

### 3.2.4 Summary

It was determined that the Spraying Systems  $\frac{1}{4}\text{J}-26\text{B}$  and  $\frac{1}{4}\text{J}-2050$ , as utilized at the AEDC, produce icing clouds over a limited range of the FAR-25 icing envelope. However, extension of the AEDC capabilities can be achieved by use of the Spraying Systems  $\frac{1}{4}\text{J}-1\text{A}$  nozzle. Use of this spray nozzle will extend the capabilities by providing clouds of lower liquid water content, and/or producing smaller MMD's than can presently be produced by the AEDC systems.

Comparison of the calibrations for the NASA-LeRC Standard nozzle and the two modified nozzles, Model I and Model II, revealed that the Model I nozzle can be used as a suitable substitute for the Standard nozzle. Utilizing the Model I in place of the Standard nozzle would provide the capability to produce low liquid water content clouds for the same range of MMD's. It was determined that the reduction in water tube diameter of the Model II nozzle was too large to provide control of the MMD's over the range required. Therefore, the Model II nozzle cannot be utilized as a substitute for the Standard nozzle.

Complete calibrations of three Sonicore nozzles were obtained. It was determined that the Sonicore #125 can be used to produce icing clouds, especially where large volumes of water are required. Also, it was found that either the Sonicore #052 or #035 can be used as an acceptable substitute for the #125 when lower flow rates are required. The slopes of the water flow calibration were found to be less steep for the Sonicore #035, thus requiring less precise control of the water pressure during testing. For this reason, the Sonicore #035 was selected as the most suitable substitute for the Sonicore #125.

### **3.3 COMPARISON OF CALIBRATIONS**

The IRT of NASA-LeRC uses 77 standard spray nozzles to produce an icing cloud. Calibration of the tunnel was accomplished utilizing rotating multicylinders and oil slides. The empirical equation for the MMD's which is based on the tunnel calibration is (Ref. 10),

$$\text{MMD} = \frac{1.09(43.9 - \sqrt{3.48 V}) \sqrt{38.7(P_w - P_a)}}{\left(\frac{P_a}{1.13} + 10\right)} + 0.0052V + 4 \quad (1)$$

where

$P_a$  = air pressure setting, psig

$P_w$  = water pressure setting, psig

$V_\infty$  = tunnel air speed, mph

$20 < P_a < 75$  psig

$P_w < 110$  psig

$5 < (P_w - P_a) < 65$  psig

Equation (1) was used to calculate MMD's for comparison with the calibration data obtained as part of this program. The air and water pressures that were in the applicable range, along with the primary air velocity, were used to calculate an MMD for the data points of Fig. 10. The calculated values became the NASA-LeRC calibration. The applicable data from Fig. 10 were then used with the NASA-LeRC calibration to plot a scatter diagram, Fig. 26.

Although the data of Fig. 26 are seen to fall on both sides of the line of perfect agreement, there is a bias toward the upper side. The bias was verified by performing a linear regression fit to the data. The resulting equation is

$$\bar{D}_{\text{AEDC}} = (1.02) \bar{D}_{\text{NASA}} + 0.54, \quad (2)$$

where

$D_{\text{AEDC}}$  = AEDC calibration of MMD,  $\mu\text{m}$

$D_{\text{NASA}}$  = NASA calibration of MMD,  $\mu\text{m}$

The maximum absolute bias is seen to exist at the largest droplet diameter, 28  $\mu\text{m}$ , and is 1.10  $\mu\text{m}$ , or 3.9 percent. The smallest absolute bias occurs for the 13- $\mu\text{m}$  size and is 0.8  $\mu\text{m}$ , or 6.2 percent.

The dashed lines of Fig. 26 illustrate the  $\pm 1 \mu\text{m}$  bandwidth around the line of perfect agreement. Sixty-five percent of the data are seen to be within the  $\pm 1 \mu\text{m}$  band.

From this analysis it is concluded that the calibration performed for a single Standard spray nozzle agrees well with the existing NASA-LeRC IRT calibration. Furthermore, it is also concluded that performing droplet size calibration on single spray nozzles is a viable method, and that once a complete calibration of a nozzle has been obtained, it can be used for multinozzle spray bars. Therefore, a droplet size calibration of a spray system is not required after changing the number and location of the spray nozzles.

### 3.4 EFFECT OF VELOCITY

The effect of cell airspeed on the droplet size calibration was determined. The procedure was to hold the nozzle spray conditions constant and take droplet size measurements at incremental cell airspeeds. The effects were determined for three nozzles, the SS $\frac{1}{4}$ J-2050, NASA-LeRC Standard, and the Sonicore #052.

Figure 27 shows the effects of cell airspeed on the calibration. The indicated droplet size is seen to be constant, and not a function of airspeed. The same airspeed independence was observed at NASA-LeRC (Ref. 10). Both findings are not in agreement with the original calibration results of the IRT. However, Olsen (Ref. 11) subsequently pointed out that the IRT calibration should be changed so that the velocity dependence is removed. Further, he recommended that Eq. (1) be evaluated at  $V_\infty = 150$  mph regardless of the actual airspeed. (This was done in the present work, but only because testing was conducted at  $V_\infty = 150$  mph.)

Based on the results it was concluded that the cell airspeed had no effect on the calibration.

### 3.5 NATURAL ICING CLOUD COMPARISONS

A natural icing cloud is a collection of supercooled water droplets that is continually changing. The changes occur in the droplet size distribution, liquid water content, and temperature. Furthermore, the rate of change of these parameters varies with position within the cloud and the development stage of the cloud. Therefore, to find a single set of icing cloud data for comparison purposes is not possible.

To make a comparison between a natural icing cloud and a nozzle calibration, one must turn to an empirical expression for the size distribution of cloud droplets. A variety of empirical expressions exist and are used for this purpose (Ref. 10). The expression selected for this study takes the form

$$\begin{aligned} n(d) &= Ad^2e^{-bd} \\ &= Ad^2e^{-\frac{6d}{d_{avg}}}, \end{aligned} \quad (3)$$

where  $d$  is the droplet diameter,  $d_{avg}$  is the average diameter,  $n(d)$  is the droplet size distribution density per  $\text{cm}^3$ , and  $A$  is a constant.

It can be shown that (Ref. 12)

$$d_{avg} = \frac{1}{M} \int_0^\infty dn(d) = \frac{6}{d},$$

$$LWC = \frac{1}{6} \pi \rho_w \int_0^\infty d^3 n(d) d(d),$$

$$A = \frac{4.31(LWC) \times 10^{-15}}{(MMD)^6},$$

where  $N = \int_0^\infty n(d) d(d)$  is the total number of droplets per  $\text{cm}^3$ , and LWC is the cloud water content in  $\text{g/m}^3$ .

These equations were used to obtain the percent liquid water content contained in a given interval  $d$  to  $d + \Delta d$ . The results are shown in Fig. 28. From Fig. 28 it is seen that, in nature, the peak or mode of the distribution moves to the right (toward larger droplet diameters) as the MMD's of the cloud become larger. Also, as the mode moves toward larger droplet diameters, the area under the tail of the distribution remains small. Therefore, the majority of the water is contained in droplets around the size of the MMD.

The calibration data for each spray nozzle were reduced and plotted in the format of Fig. 28. Typical data are shown in Fig. 29. These data show that as the MMD increases, the mode does not shift toward larger droplet diameters, but rather the magnitude of the mode decreases, and the area under the tail increases.

This flattening of the distributions, although different than natural icing clouds, does not mean that the nozzles are incapable of providing an acceptable icing simulation at the large MMD's. As shown in Ref. 5, if the ground test facility provides a spray cloud with the correct MMD size and of the correct LWC, then the absolute rates of impingement of water on the aircraft components should correspond to the flight impingement rates. To ensure that this is indeed the case, however, each aircraft component, especially those that are critical during an icing encounter, should be analyzed before testing, using the techniques outlined in Ref. 5 and the calibration data of this report.

#### **4.0 CONCLUSIONS AND RECOMMENDATIONS**

An experimental study of ten spray nozzles was conducted to extend the icing testing capabilities of the AEDC, and to determine the requirements for atomizer calibration. It was determined that the Spraying System nozzles used by the AEDC produce icing clouds over a limited range of the FAR-25 icing envelope. However, the icing simulation capabilities of the AEDC can be extended by use of a Spraying System  $\frac{1}{4}$ J-1A nozzle. Both the liquid water content of the clouds and the resulting mass median diameter can be reduced by utilizing the nozzle. It is recommended that provisions be made to incorporate the SS $\frac{1}{4}$ J-1A nozzle in the AEDC spray nozzle inventory and that the operational procedures required to use it be developed.

Comparison of the calibration results obtained for a single nozzle with the NASA-LeRC calibration of 77 nozzles led to the conclusion that performing droplet size calibrations on a

single spray nozzle is a viable technique. Also, once a complete calibration of a nozzle has been obtained, it can be used for multinozzle spray bars. Therefore, a droplet size calibration of a spray system is not required after changing the number and/or location of the spray nozzles.

A study of the effects of velocity on the three types of spray nozzle (internal, external, and sonic mixing nozzles) calibration was made. Based on these results, it was concluded that cell airspeed had no effect on the spray nozzle calibrations.

An empirically derived function was used to obtain theoretical droplet size distribution for a natural icing cloud. The theoretical results were compared to the distributions obtained as part of this study. It was determined from the comparison that the distribution obtained for the spray nozzles did not agree with the natural icing cloud distribution as the MMD's became large. To overcome this discrepancy, it is recommended that the critical aircraft components be analyzed before testing to determine the influence of the difference between the distribution. The data obtained as part of this study will be invaluable to the analysis.

Comparison of the calibrations for the NASA-LeRC Standard nozzle and the two modified nozzles, Model I and Model II, revealed that the Model I nozzle can be used as a suitable substitute for the Standard nozzle. Use of the Model I as a substitute for the Standard nozzle would provide simulated icing clouds with lower LWC's for the same range of MMD's. It was concluded that the Model II nozzle is not an acceptable substitute for the Standard nozzle.

## REFERENCES

1. Federal Aviation Administration. "Airworthiness Standards: Transport Category Airplanes, Appendix C." *Federal Aviation Regulation*, Part 25.
2. Olsen, William. "Survey of Aircraft Icing Simulation Test Facilities in North America." NASA-TM-81707, February 1981.
3. Hunt, Jay D. "A Comparison of Particle Diagnostic Systems." AEDC-TR-80-33 (AD-A104027), August 1981.
4. Bentley, H. T. "Fiber Optics Particle-Sizing System." AEDC-TR-73-111 (AD766647), September 1973.

5. Willbanks, C. E. and Schulz, R. J. "Analytical Study of Icing Simulation for Turbine Engines in Altitude Test Cells." AEDC-TR-73-144 (AD770069), November 1973.
6. Stallabrass, J. R. "Procedure for Allowing for the Evaporation from Water Droplets in an Engine Icing Test Cell." National Research Council of Canada (NRC) Report, LTR-LT-123, January 1982.
7. Bigg, F. J. "The Atomization of Water by Air Blast Nozzles for the Simulation of Cloud Conditions for Icing Research." RAE-TN-ME203, June 1955.
8. Abernethy, R. B., et al., Pratt and Whitney Aircraft, and Thompson, J. W. Jr., ARO, Inc. "Handbook, Uncertainty in Gas Turbine Measurements." AEDC-TR-73-5 (AD755356), November 1973.
9. Spraying System Company, Industrial Catalog 27, pp. 46-53, Wheaton, Illinois, 1978.
10. Tabeuchi, D. M., et al. "Comparison of Modern Icing Cloud Instruments." MRI-82FR-1862. Meteorology Research, Inc., February 24, 1982.
11. Olsen, W., et al. "Experimental Comparison of Icing Cloud Instruments." AIAA Paper 83-0025, Reno, Nevada, January 1983.
12. Borovikow, A. M., et al. *Cloud Physics*, Translated from Russian, Israel Program for Scientific Translations, Jerusalem, 1963.

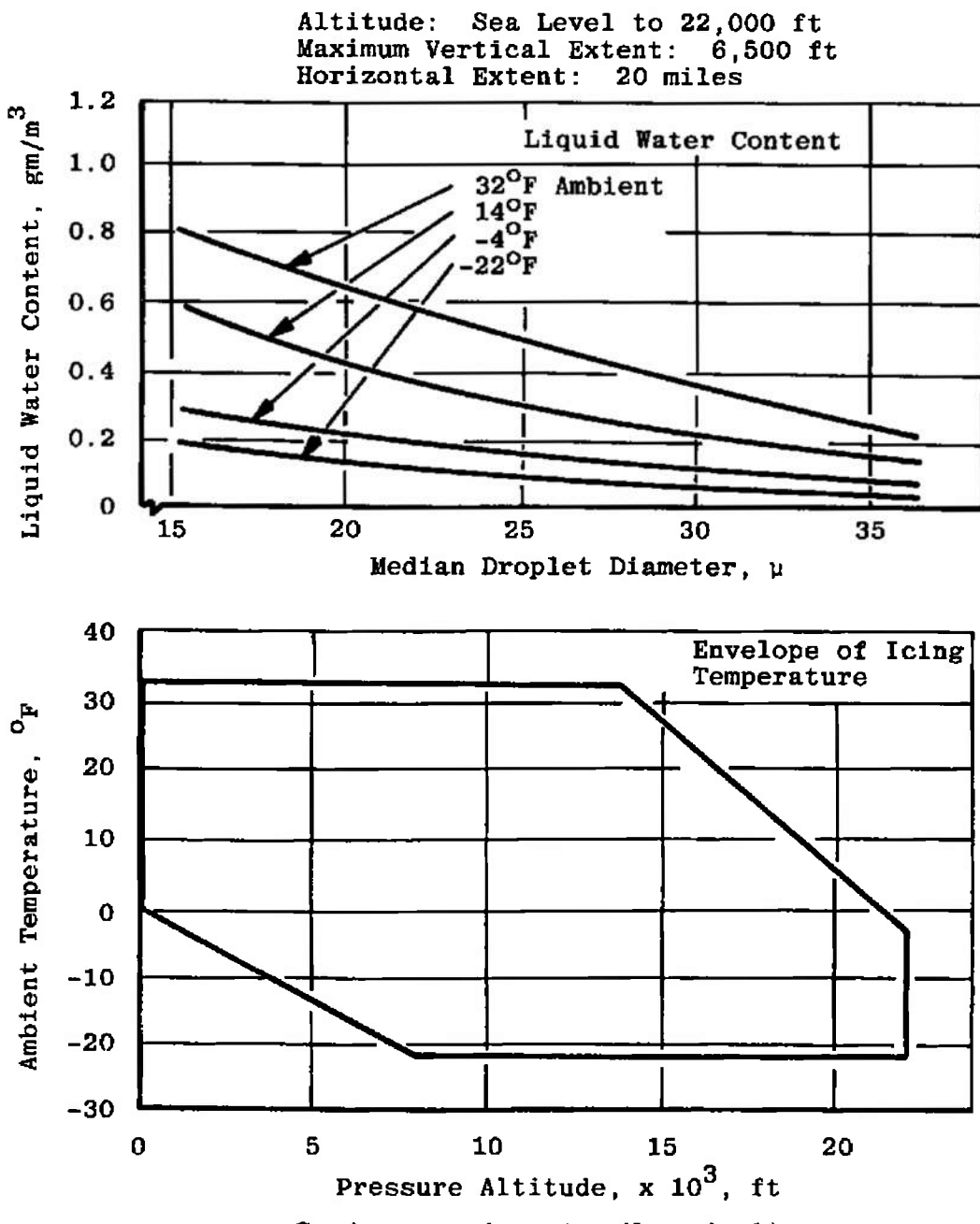
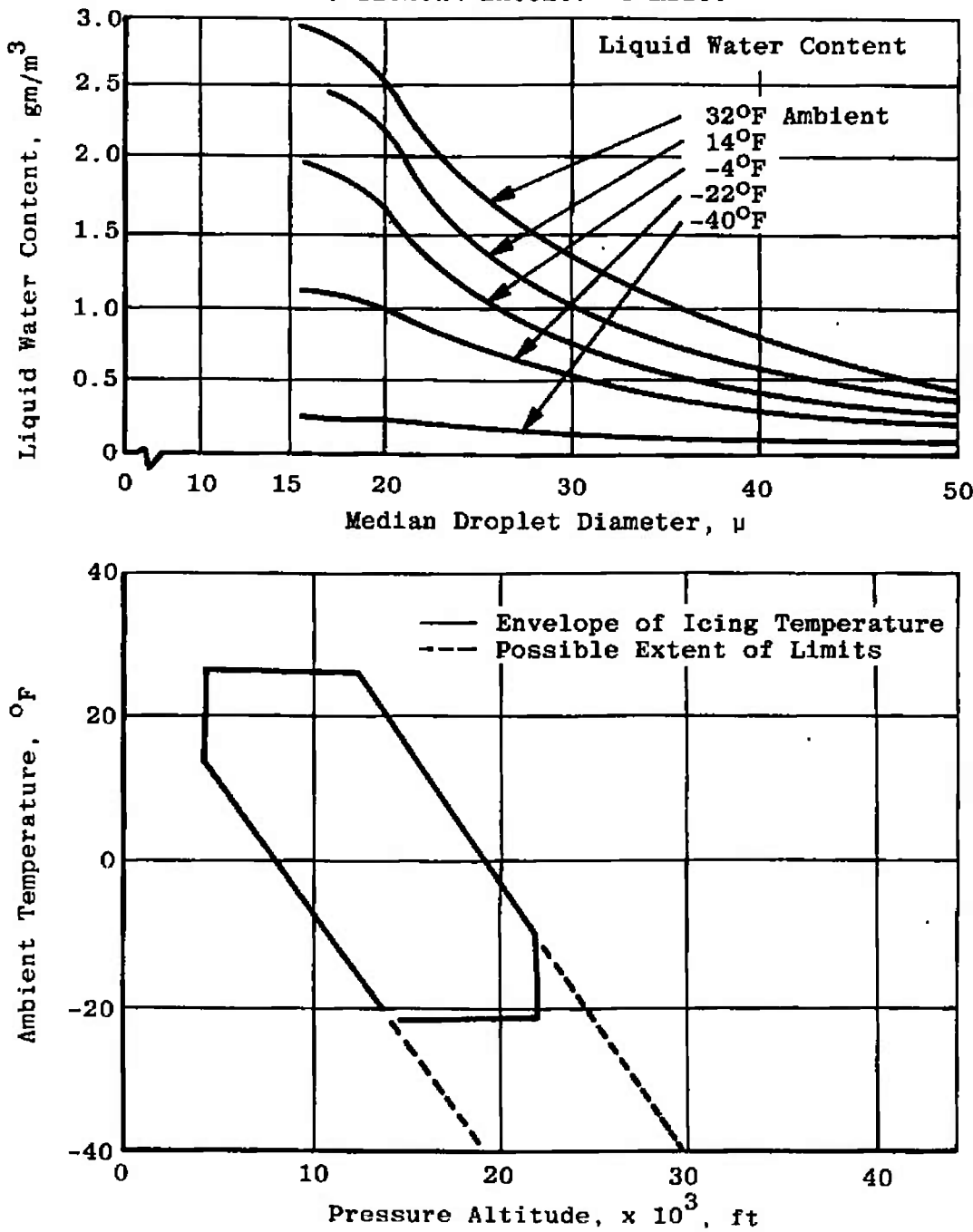
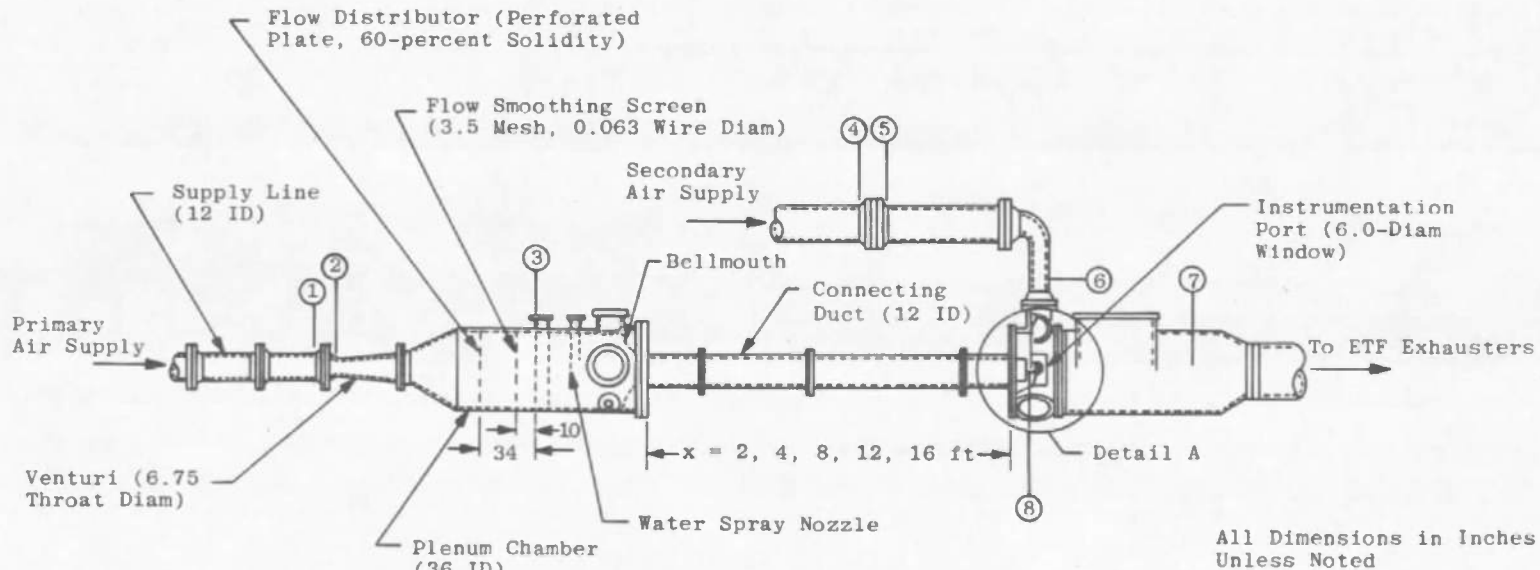


Figure 1. Cloud icing condition.

Altitude: 4,000 to 22,000 ft  
 Horizontal Extent: 3 miles



b. Intermittent maximum (cumuliform clouds)  
 Figure 1. Concluded.

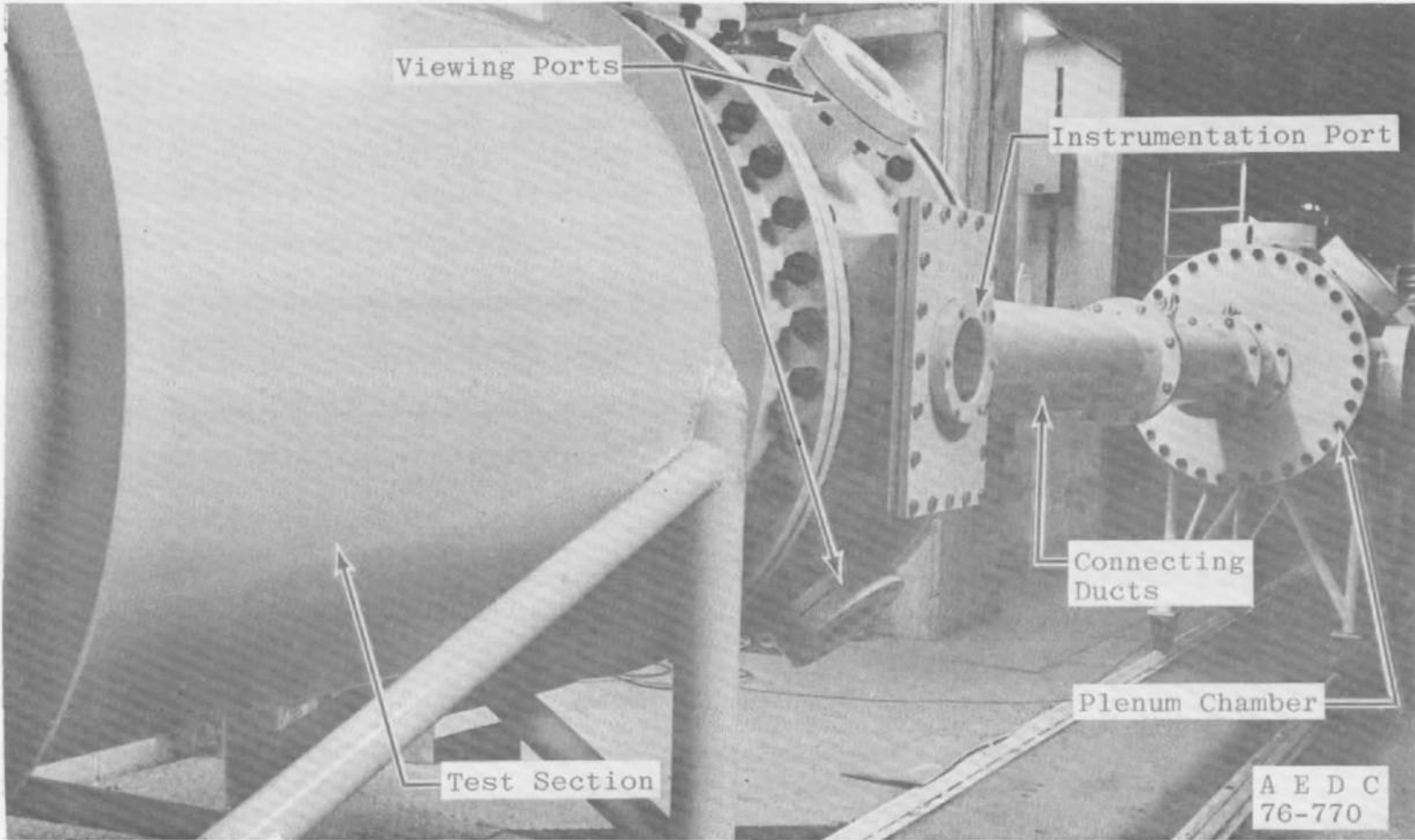


Cell Instrumentation Locations

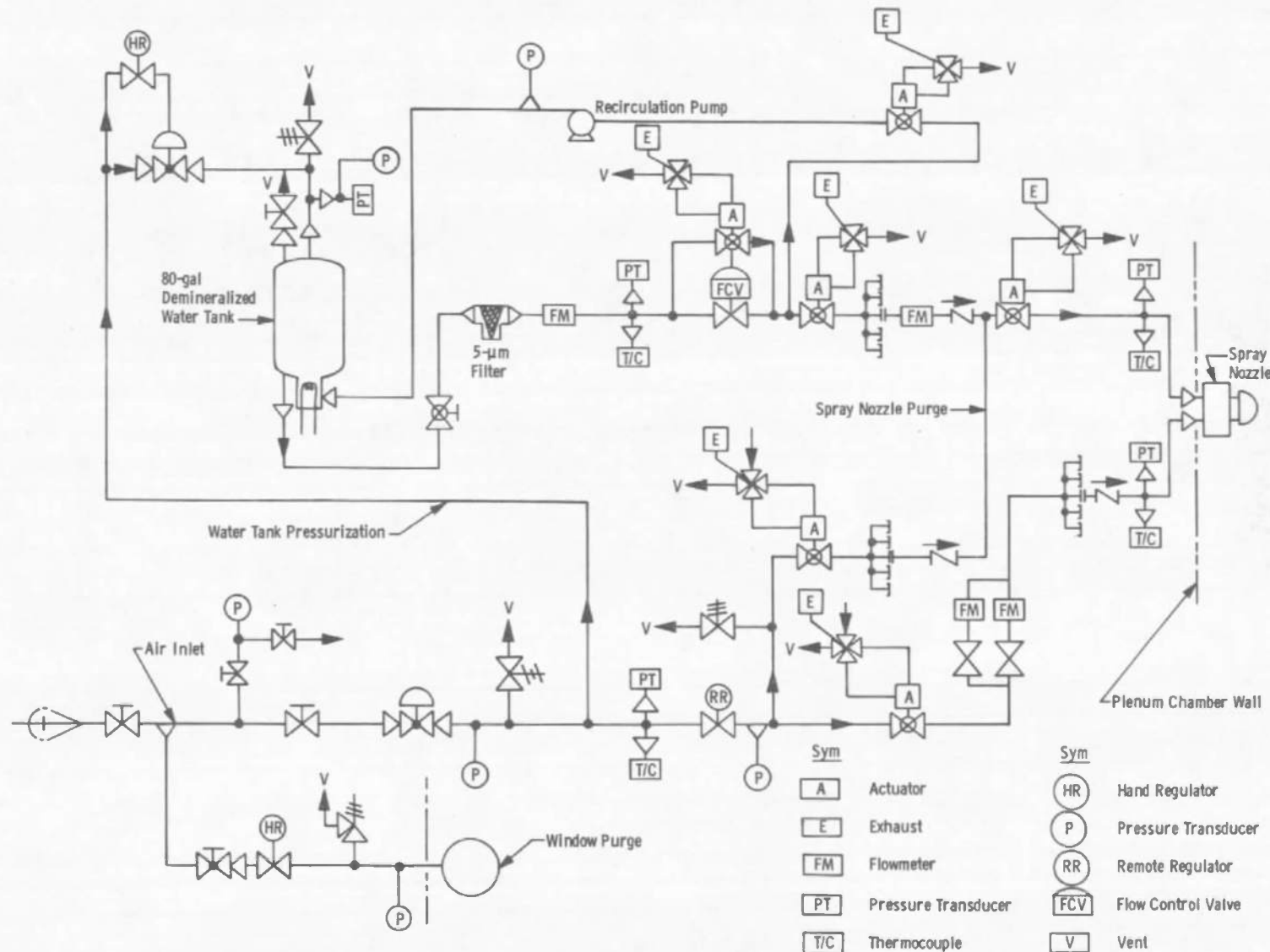
Sta	$P_t$	$P_s$	$T_t$
1	--	1	1
2	--	1	--
3	10	--	10
4	--	1	--
5	--	1	--
6	--	1	--
7	--	1	--
8	--	4	--
9	1	--	1

Detail A

a. Schematic of general layout  
 Figure 2. Icing research test cell.



b. Icing research test cell looking upstream  
Figure 2. Continued.



c. Schematic icing spray system data  
Figure 2. Concluded.

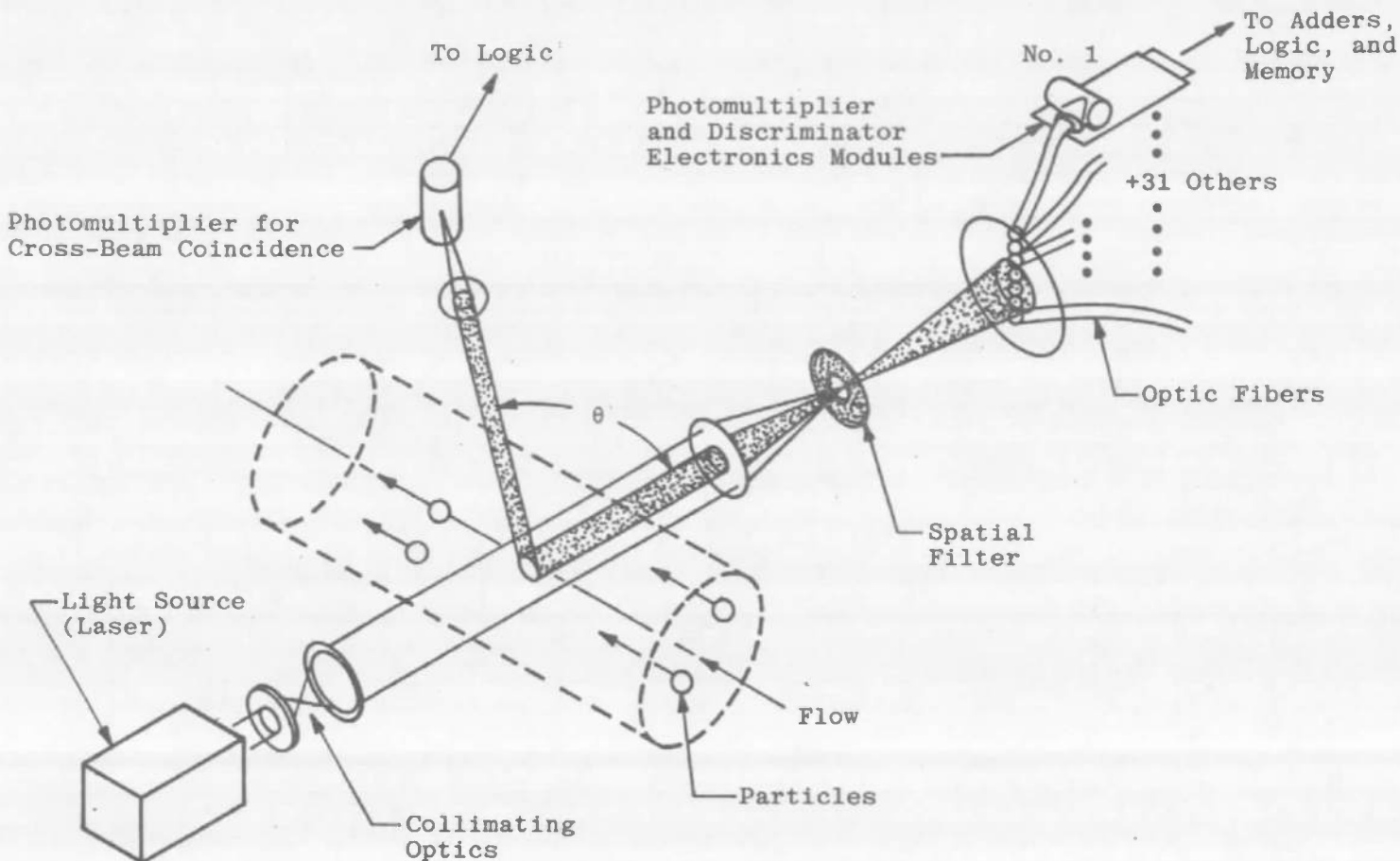


Figure 3. Fiber-optics particle-sizing system.

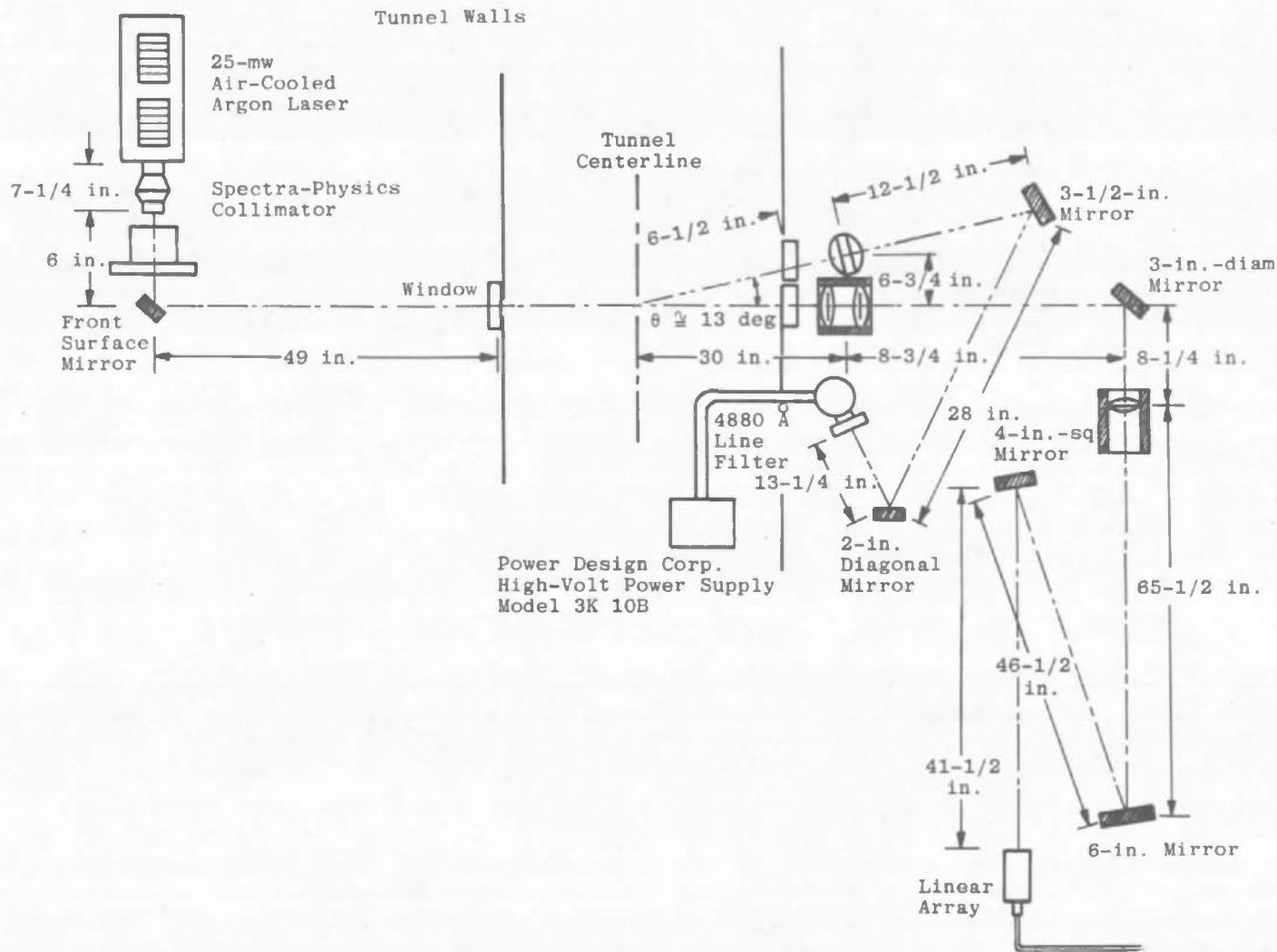
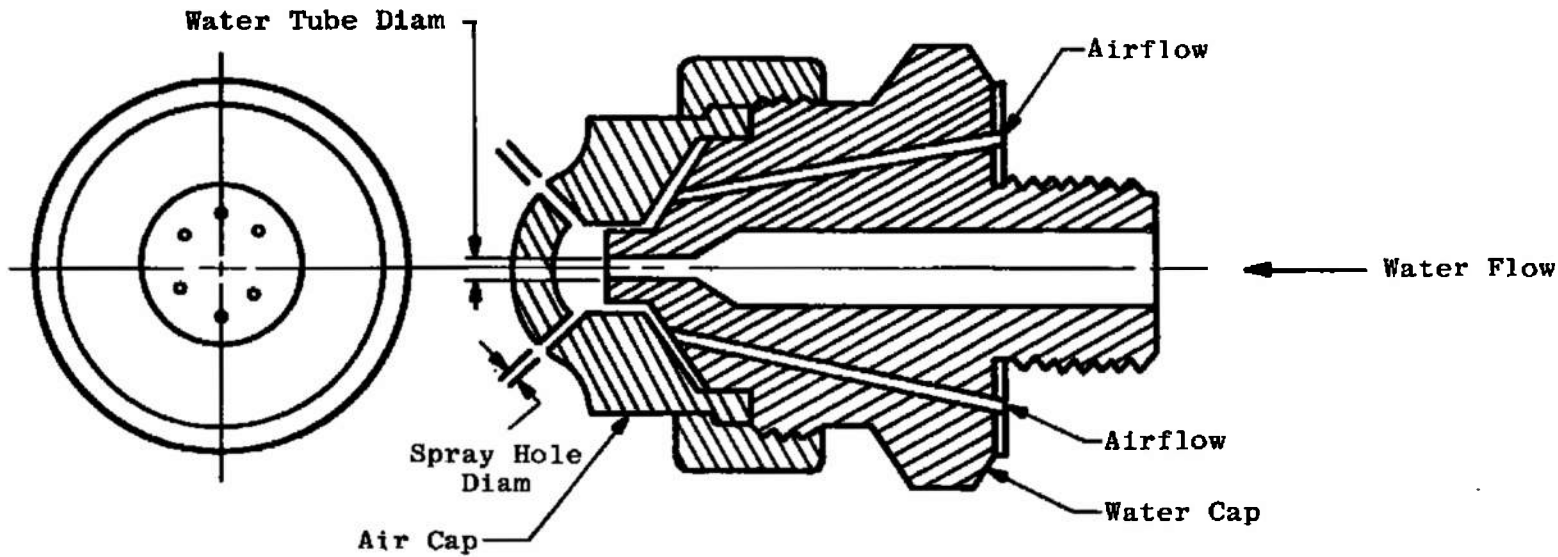


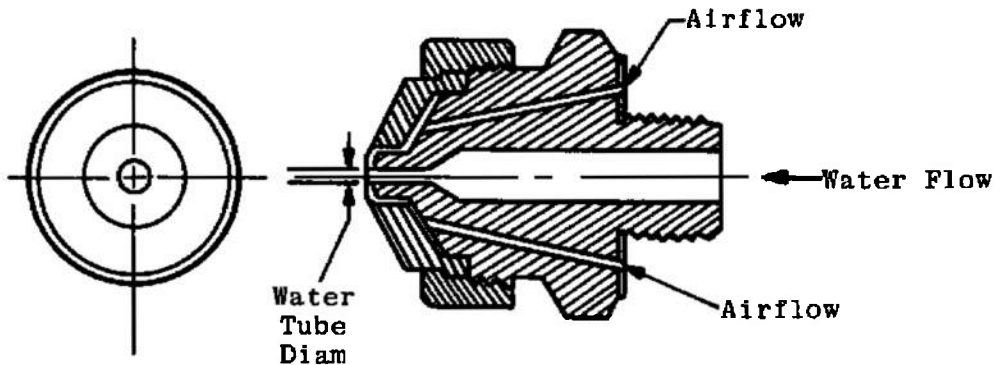
Figure 4. FOS optical arrangement.



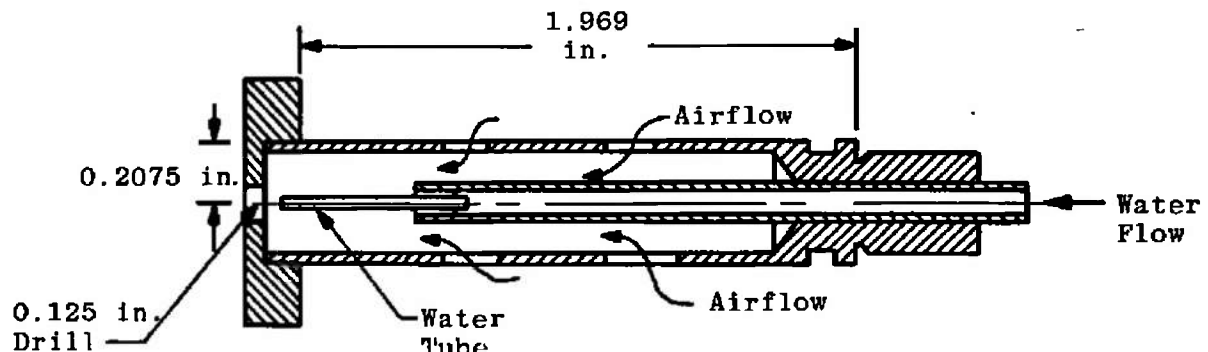
Nozzle	Air Cap No.	Water Cap No.	Water Tube I.D.	Spray Hole Diam
SS½J-26B	140-6-37-70°	40100	0.040	0.035
SS½J-2050	140-6-37-70°	2050	0.020	0.035

a. Internal mixing nozzles

Figure 5. Spray nozzles.

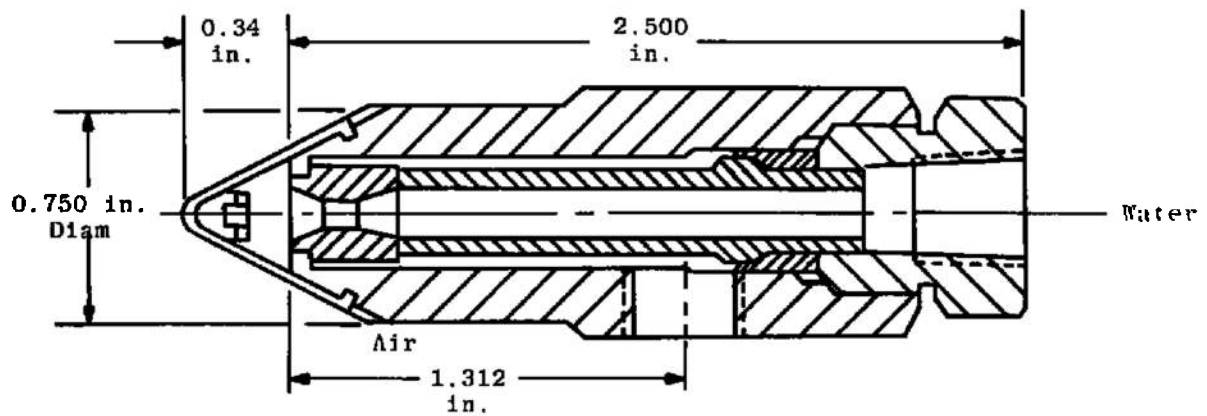


Nozzle	Air Cap No.	Water Cap No.	Water Tube I.D.	Spray Hole Diam
SS <sub>1/2</sub> J-1A	64	1050	0.010	0.064
SS <sub>1/2</sub> J-1	150	2050	0.020	0.150



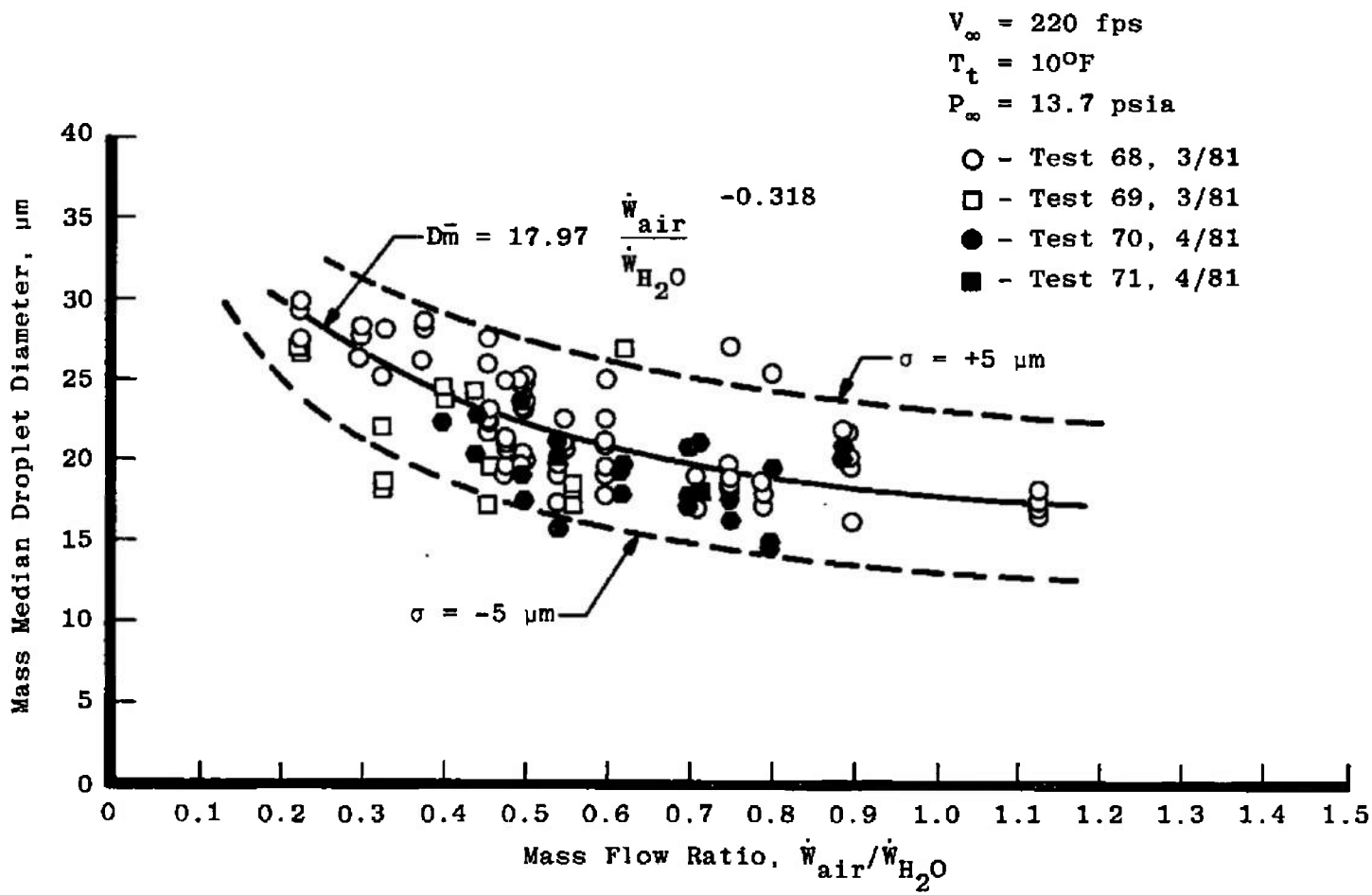
Nozzle	Water Tube I.D., in.
NASA Lewis Standard	0.025
NASA Lewis Model I	0.0155
NASA Lewis Model II	0.0102

b. External mixing nozzles  
Figure 5. Continued.



Nozzle	Water Orifice Diam	Air Bore
Sonicore 035	0.020	0.035
Sonicore 052	0.032	0.052
Sonicore 125	0.043	0.125

c. Sonic mixing nozzles  
Figure 5. Concluded.



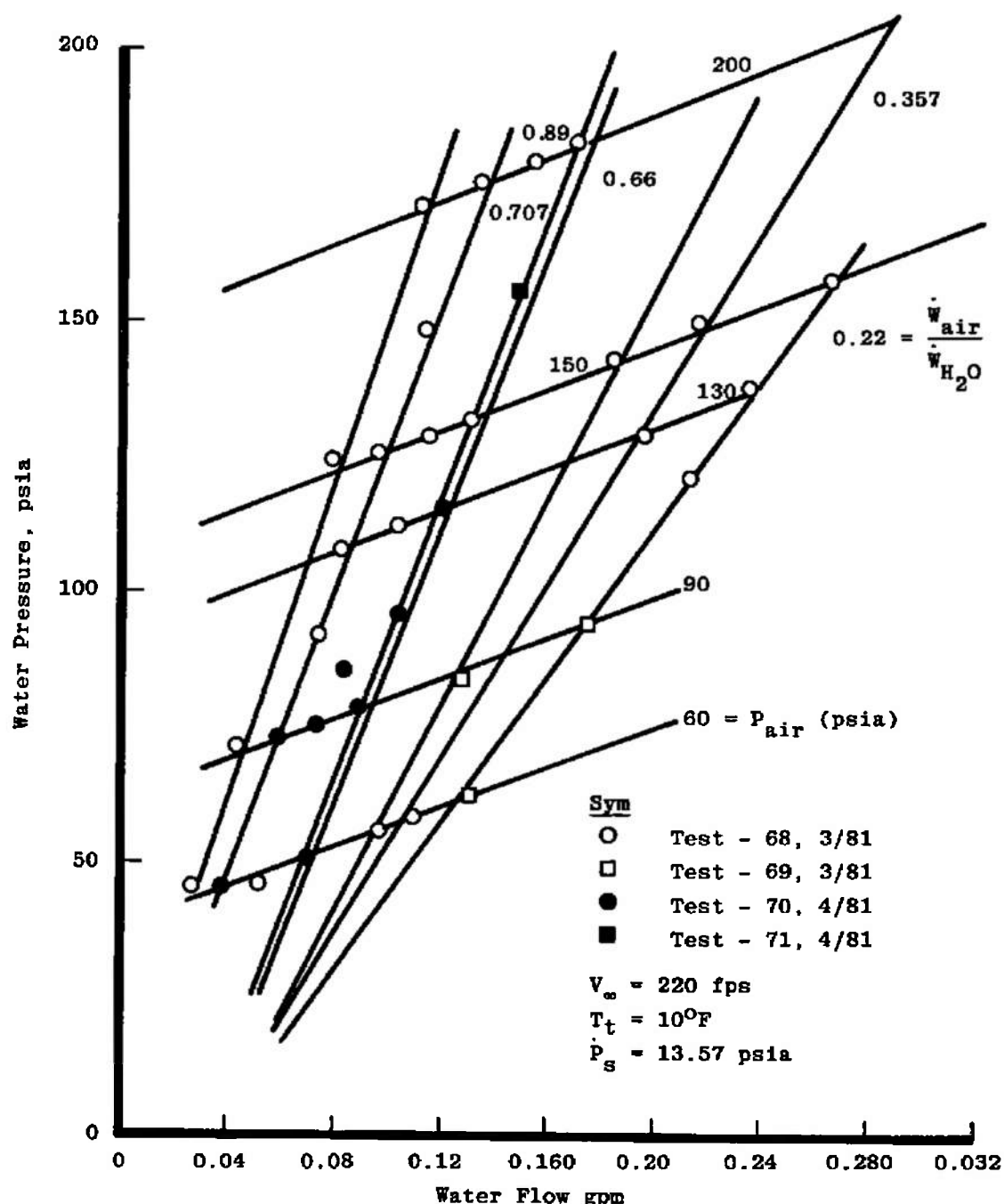


Figure 7. Water flow calibration, SS 1/4 J-26B Nozzle.

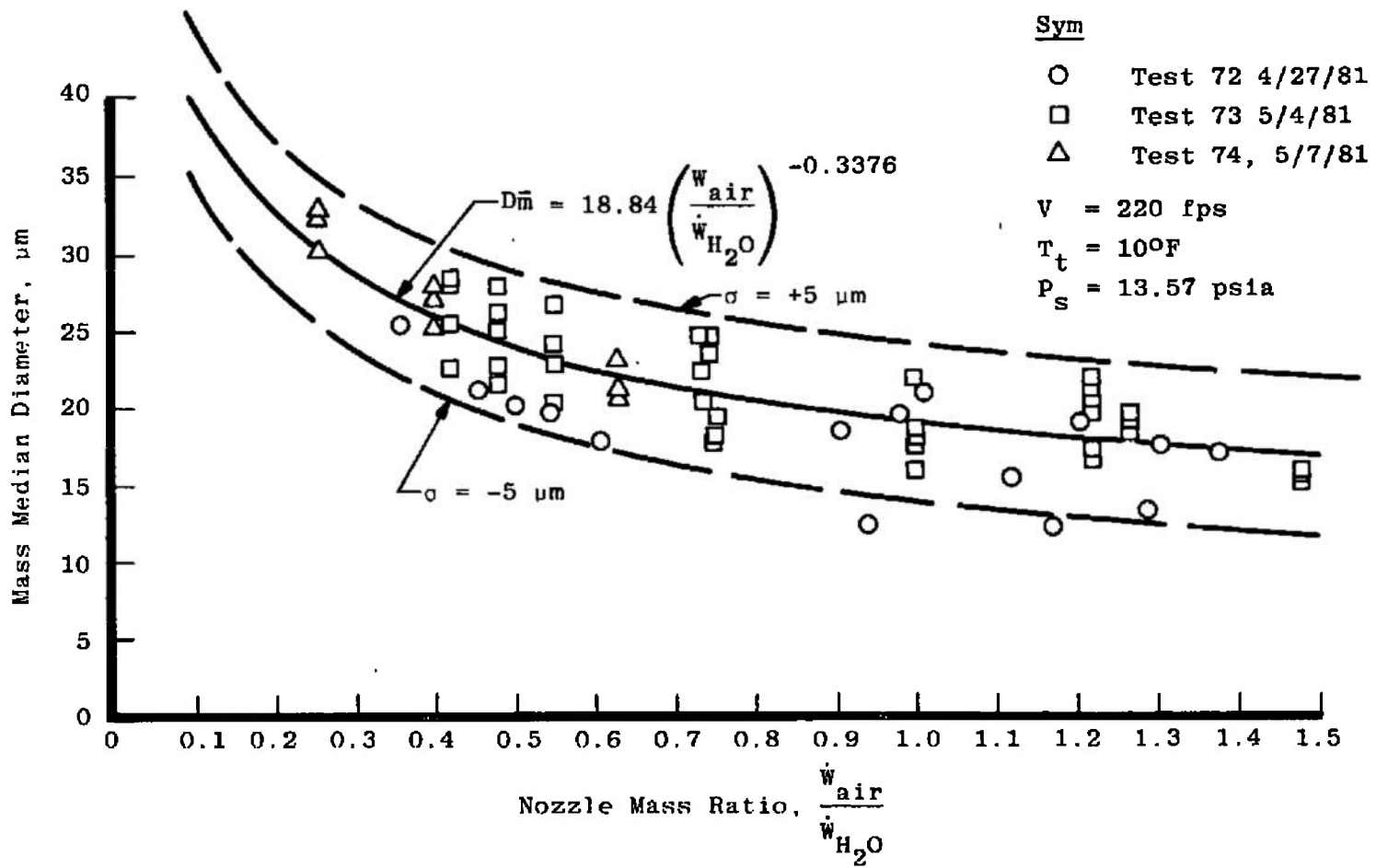


Figure 8. Droplet size calibration, SS $\frac{1}{4}$ J-2050 Nozzle.

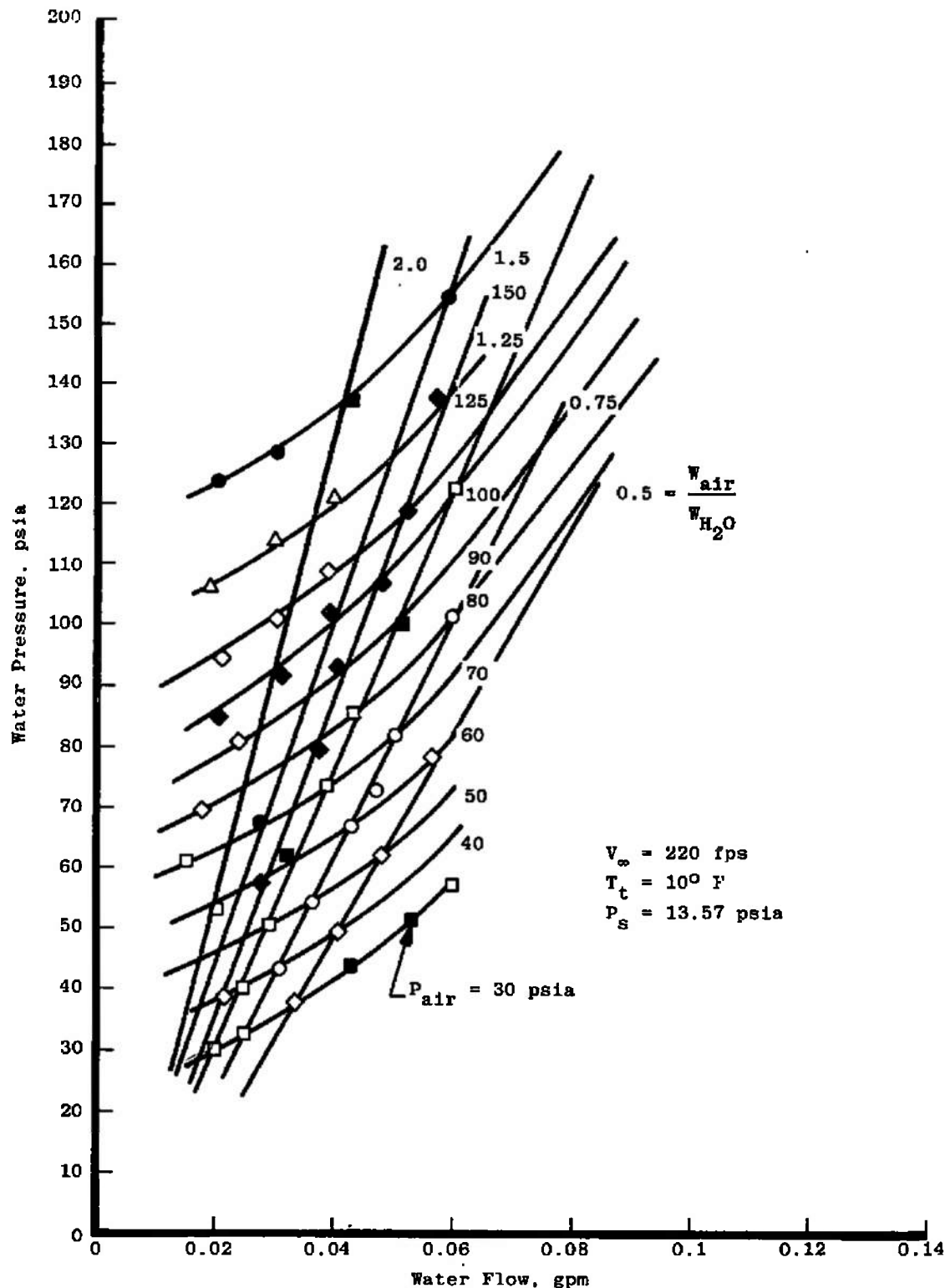


Figure 9. Water flow calibration, SS 1/4J-2050 Nozzle.

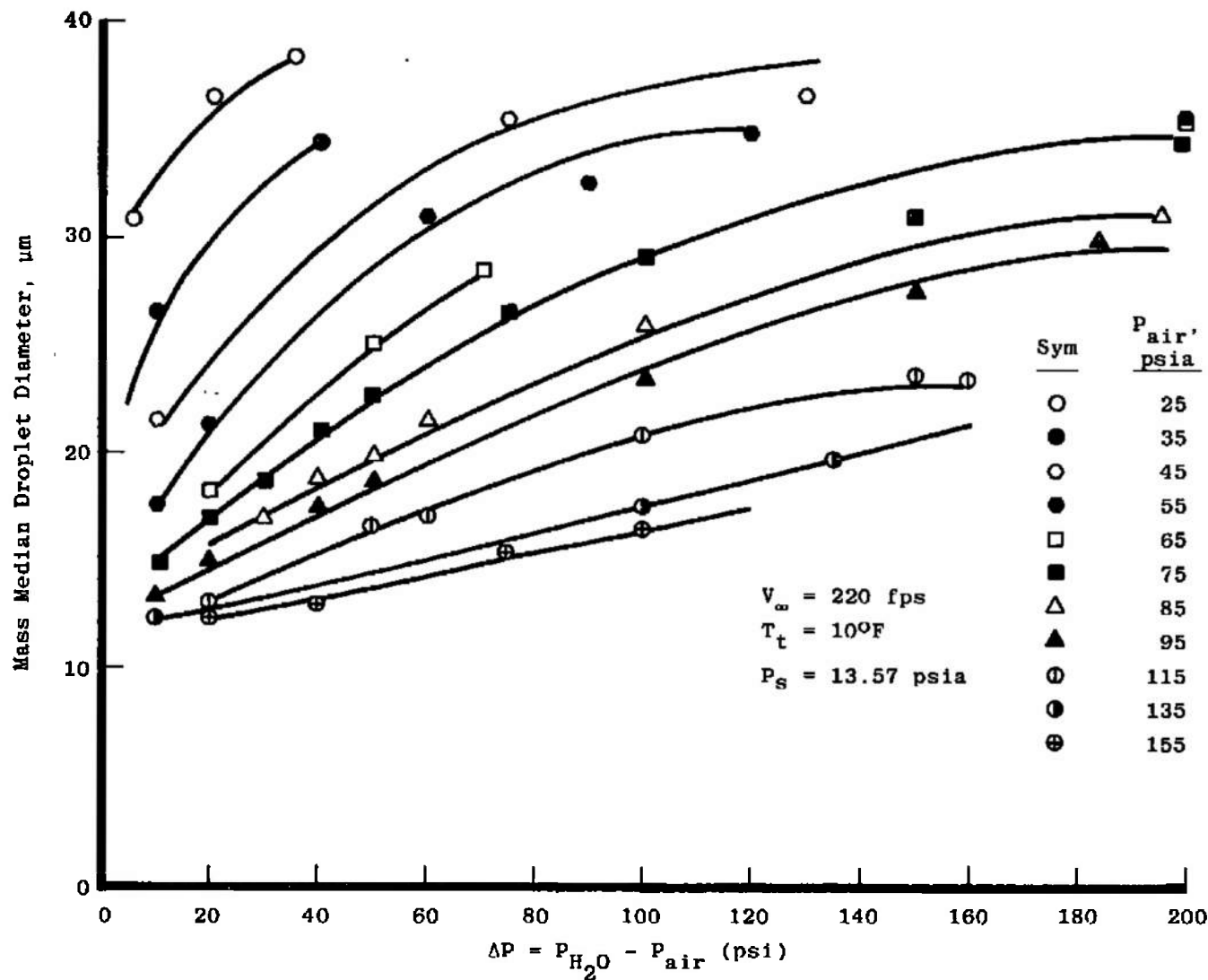


Figure 10. Droplet size calibration, NASA LeRC Standard Nozzle.

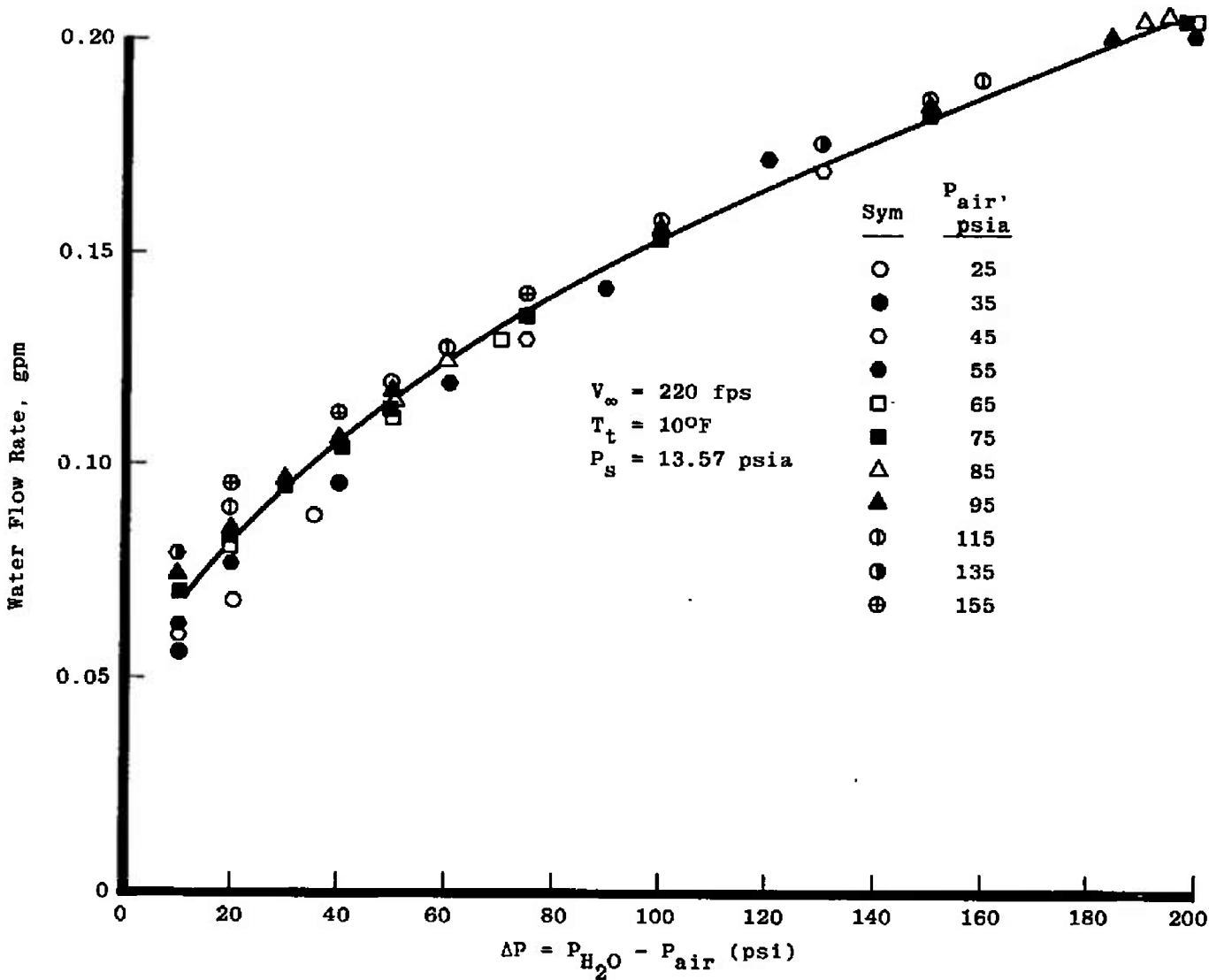


Figure 11. Water flow calibration, NASA LeRC Standard Nozzle.

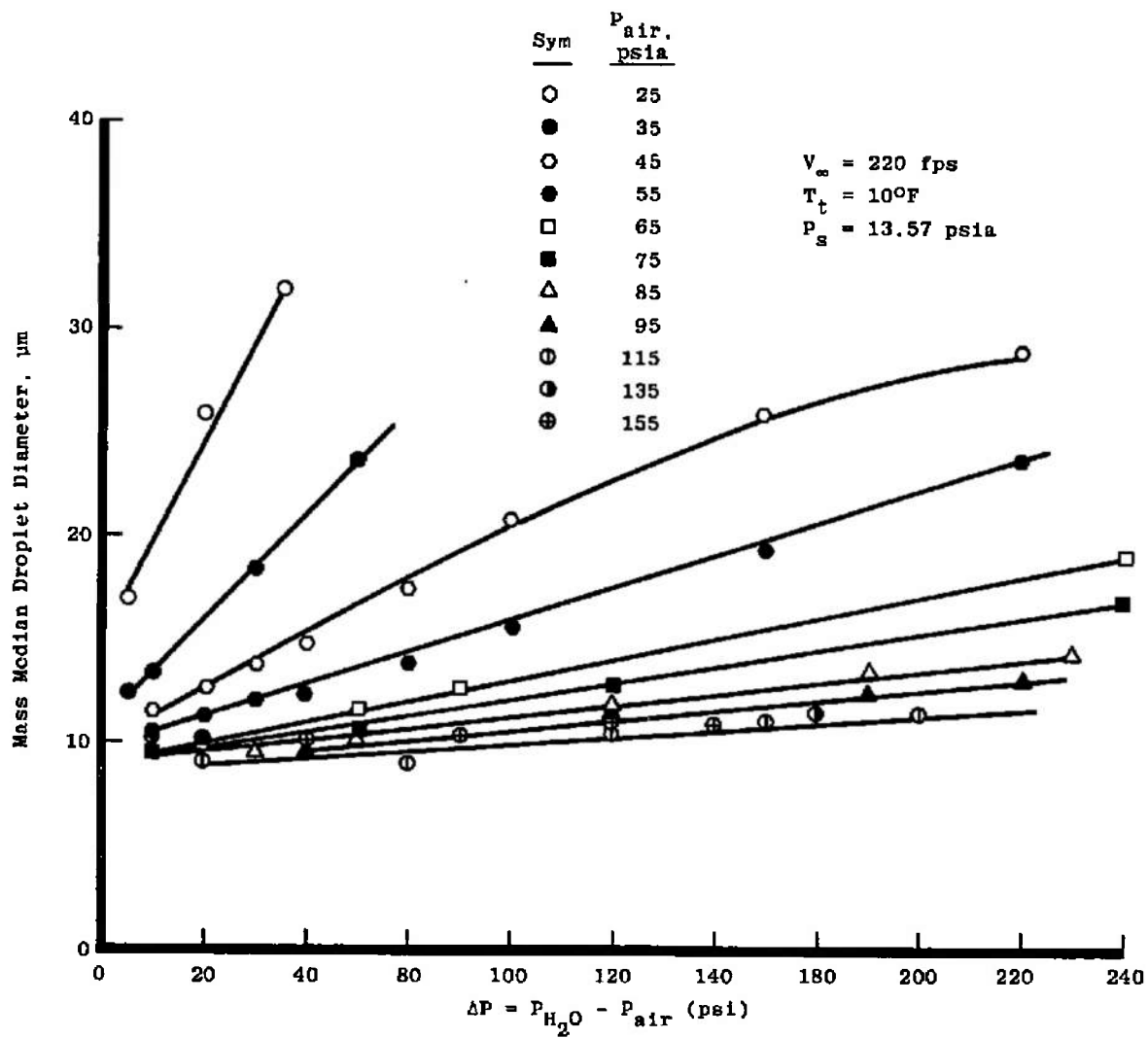


Figure 12. Droplet size calibration, NASA LeRC Model I Nozzle.

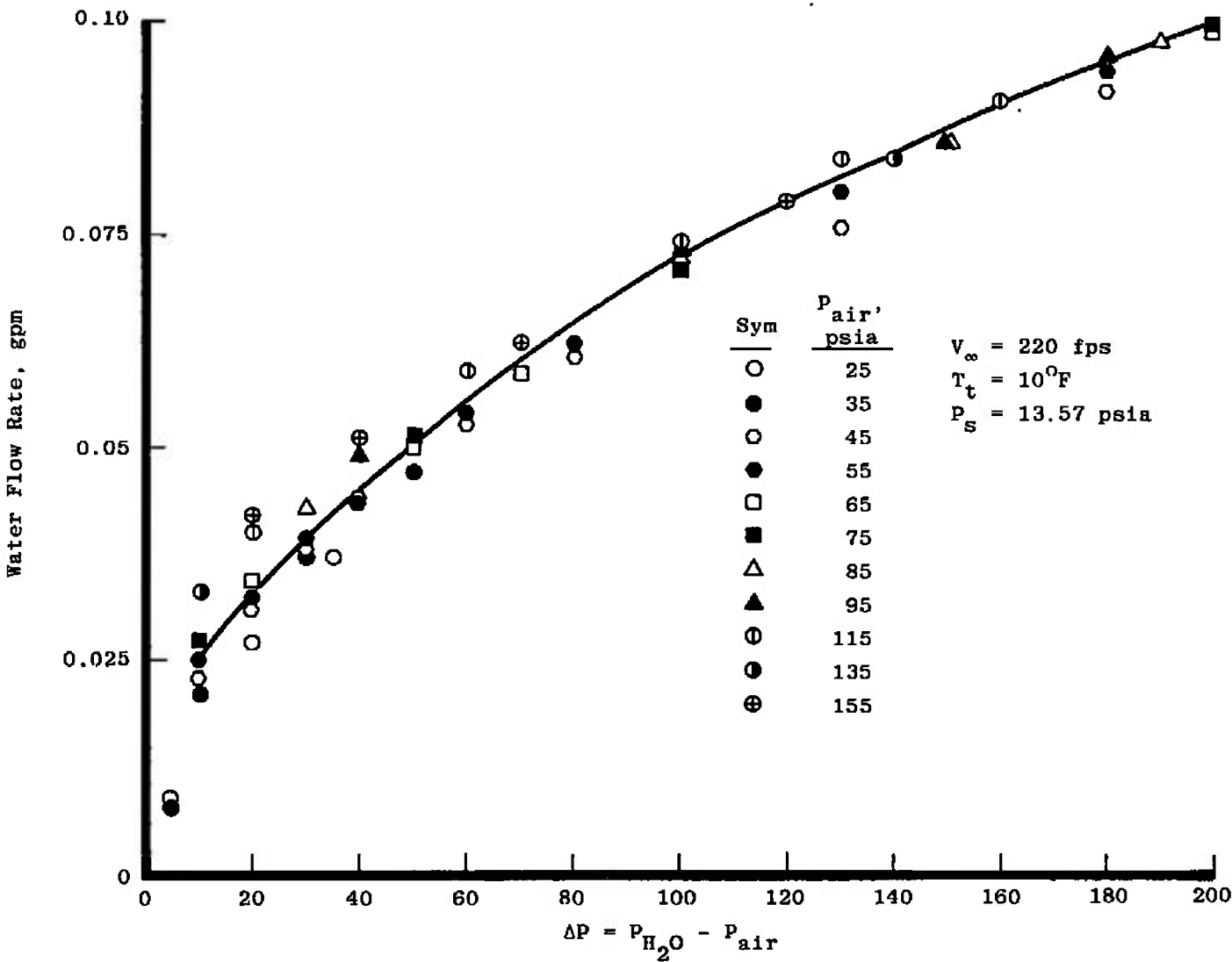


Figure 13. Water flow calibration, NASA-LeRC Model I Nozzle.

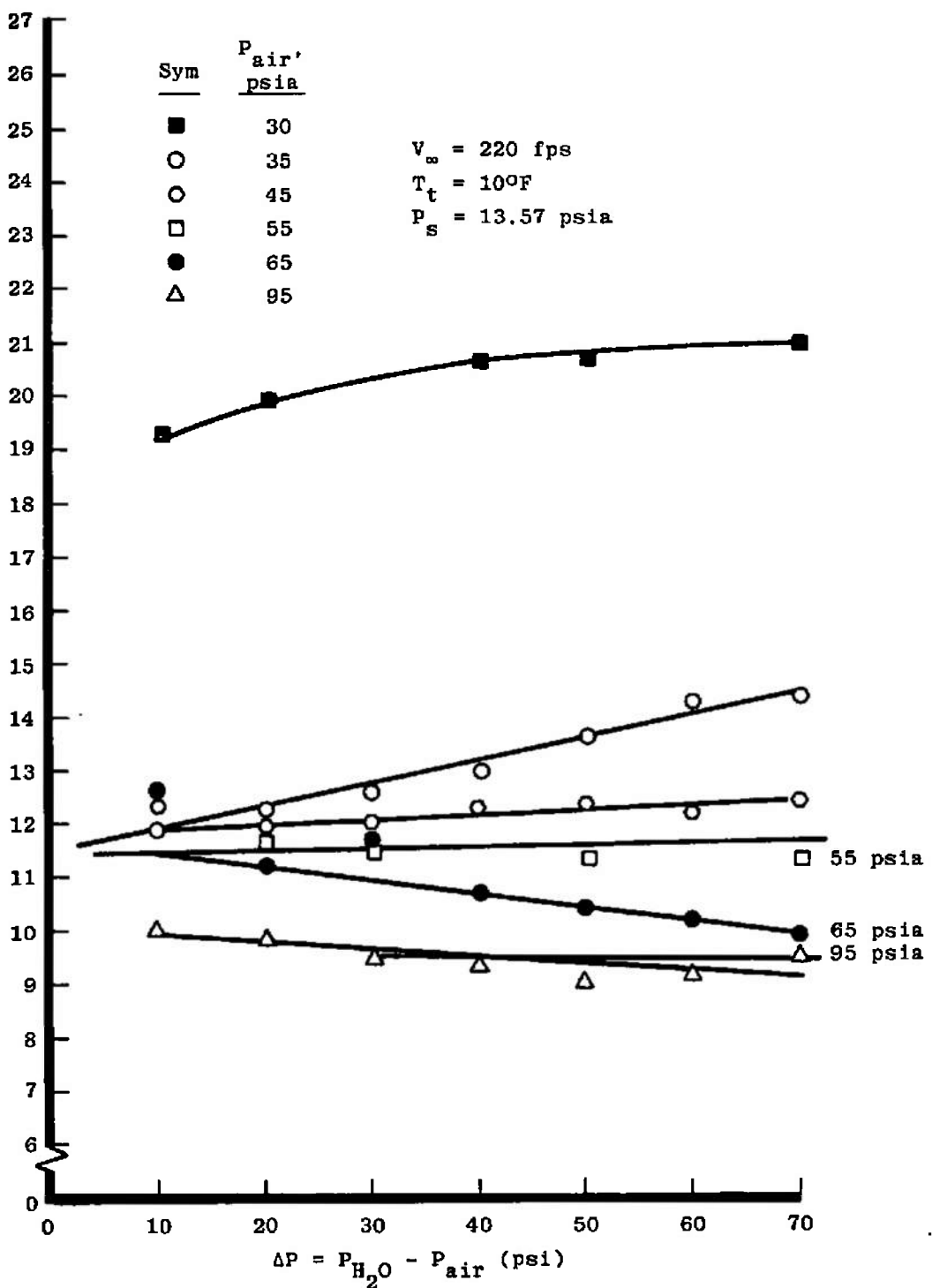


Figure 14. Droplet size calibration, NASA-LeRC Model II Nozzle.

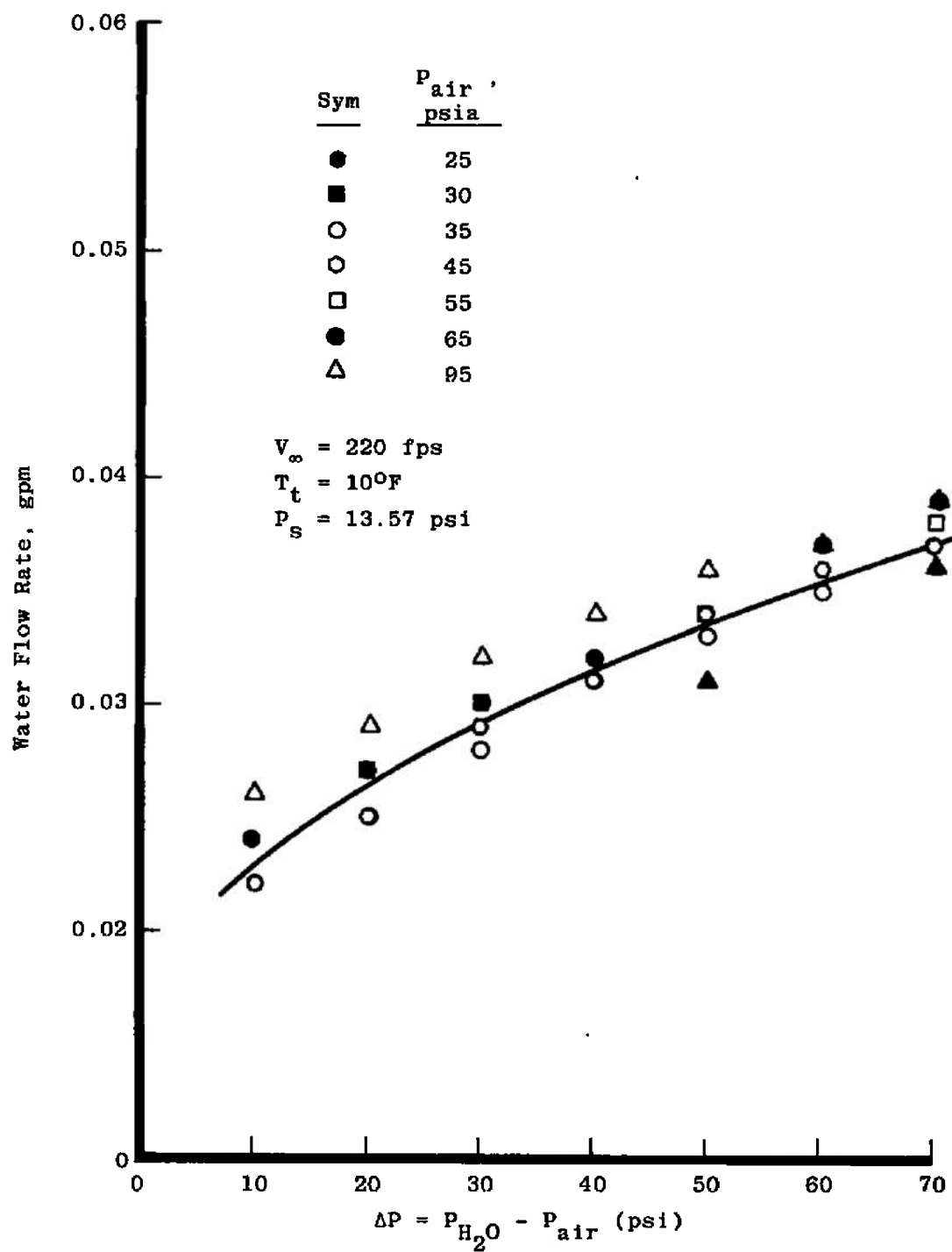


Figure 15. Water flow calibration, NASA-LeRC Model II Nozzle.

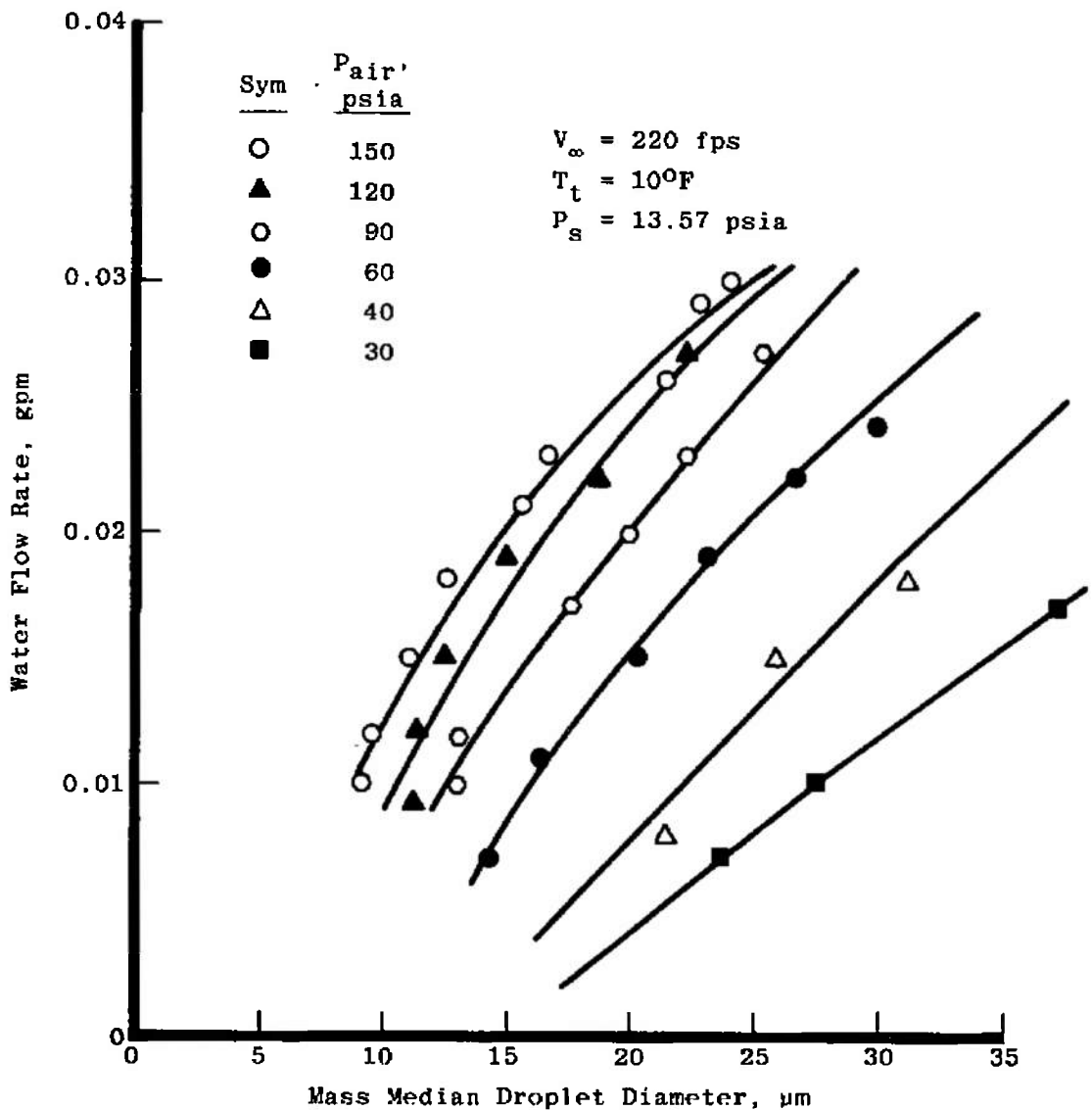


Figure 16. Droplet size calibration, SS 1/4 J-1A Nozzle.

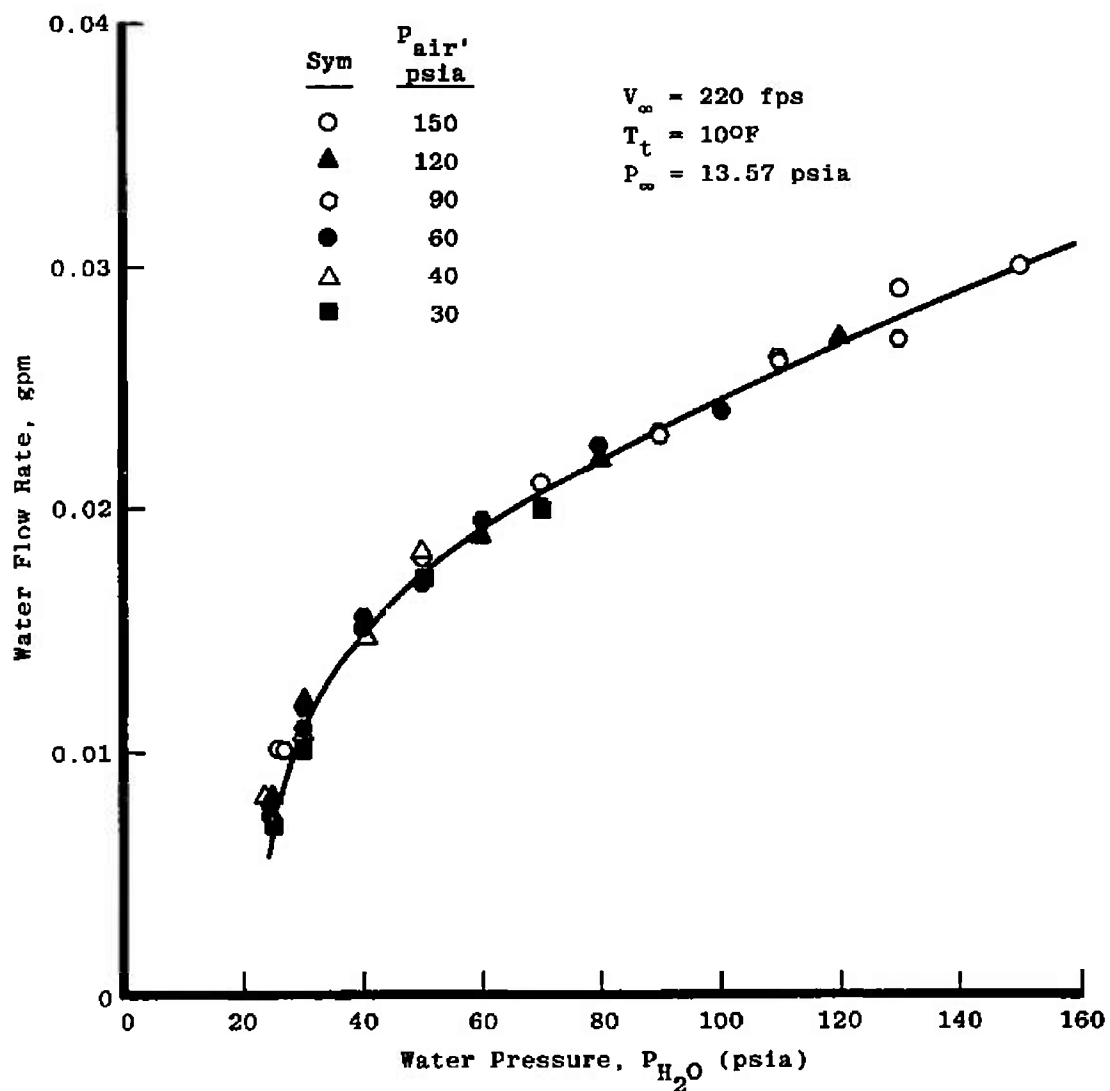


Figure 17. Water flow calibration, SS 1/4J-1A Nozzle.

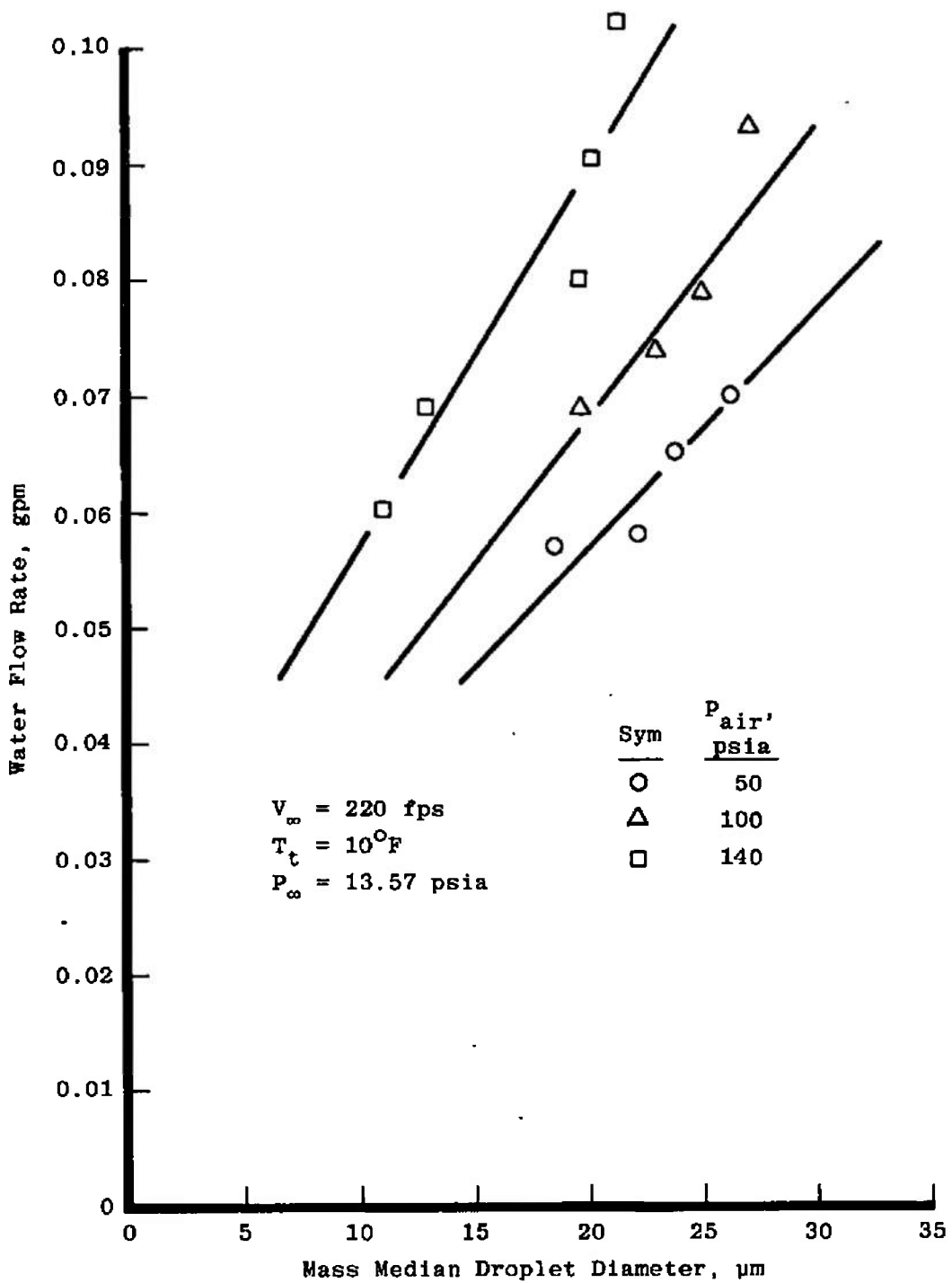


Figure 18. Droplet size calibration, SS 1/4 J-1 Nozzle.

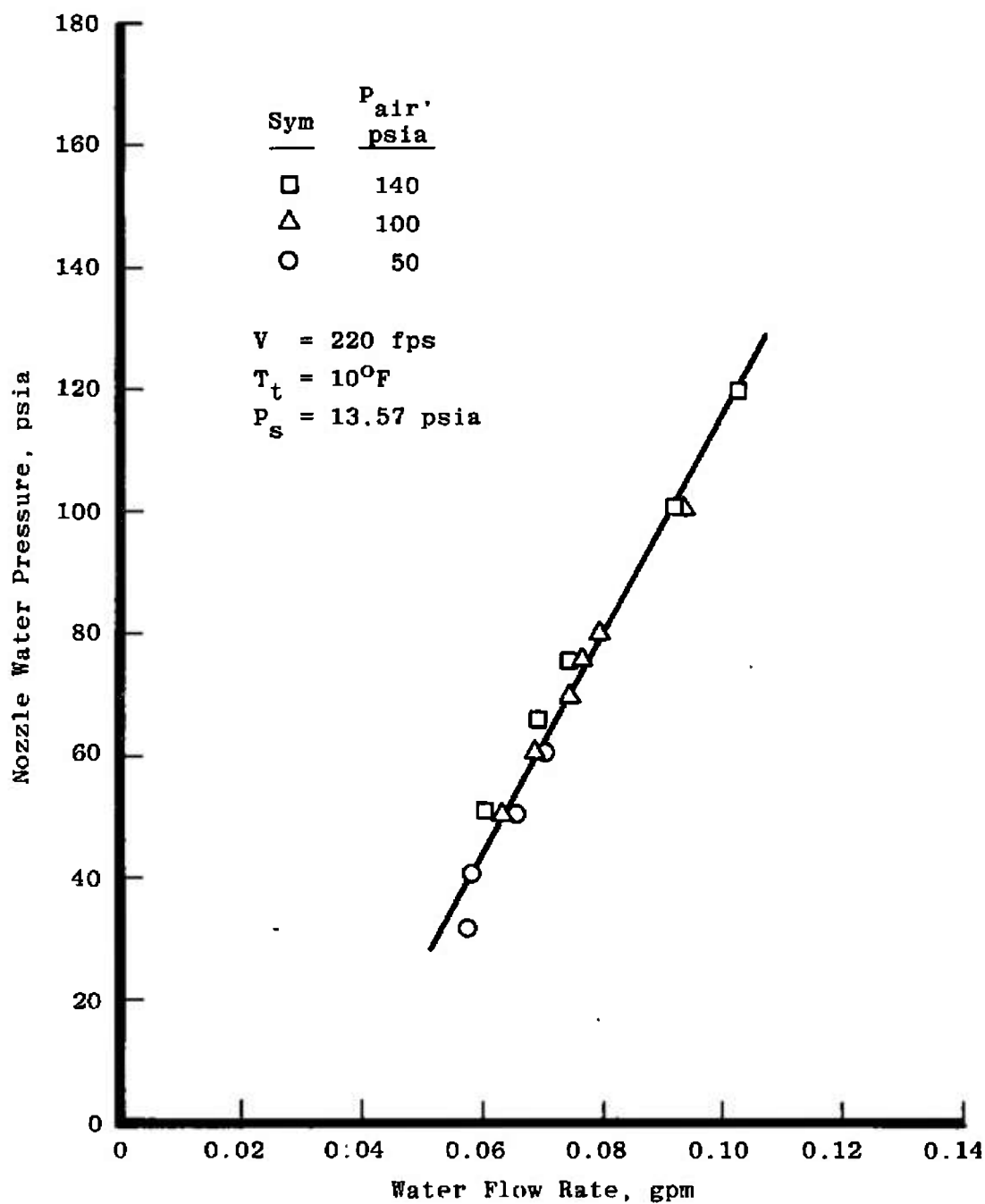


Figure 19. Water flow calibration, SS 1/4 J-1 Nozzle.

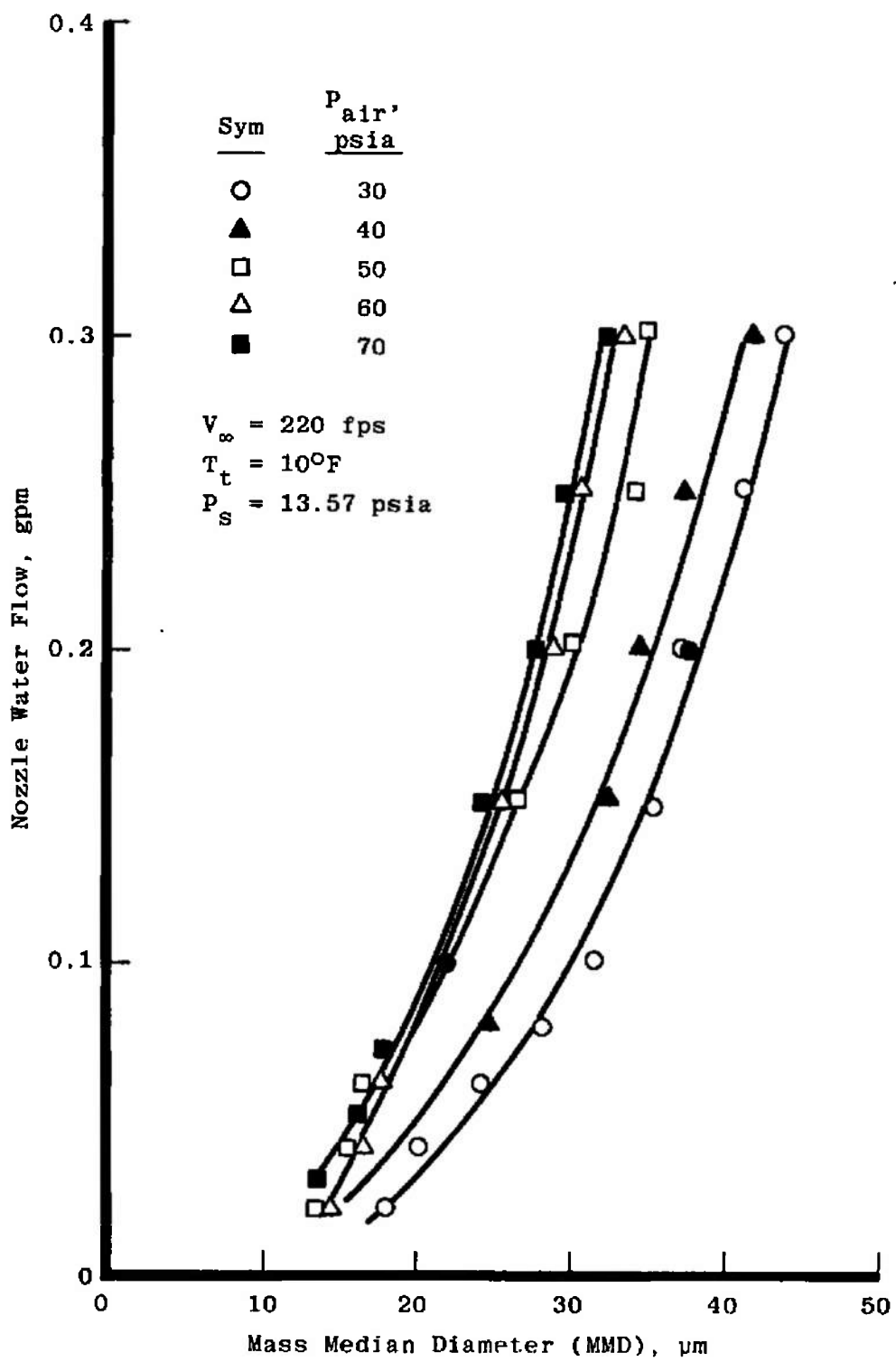


Figure 20. Droplet size calibration, Sonicore #125 Nozzle.

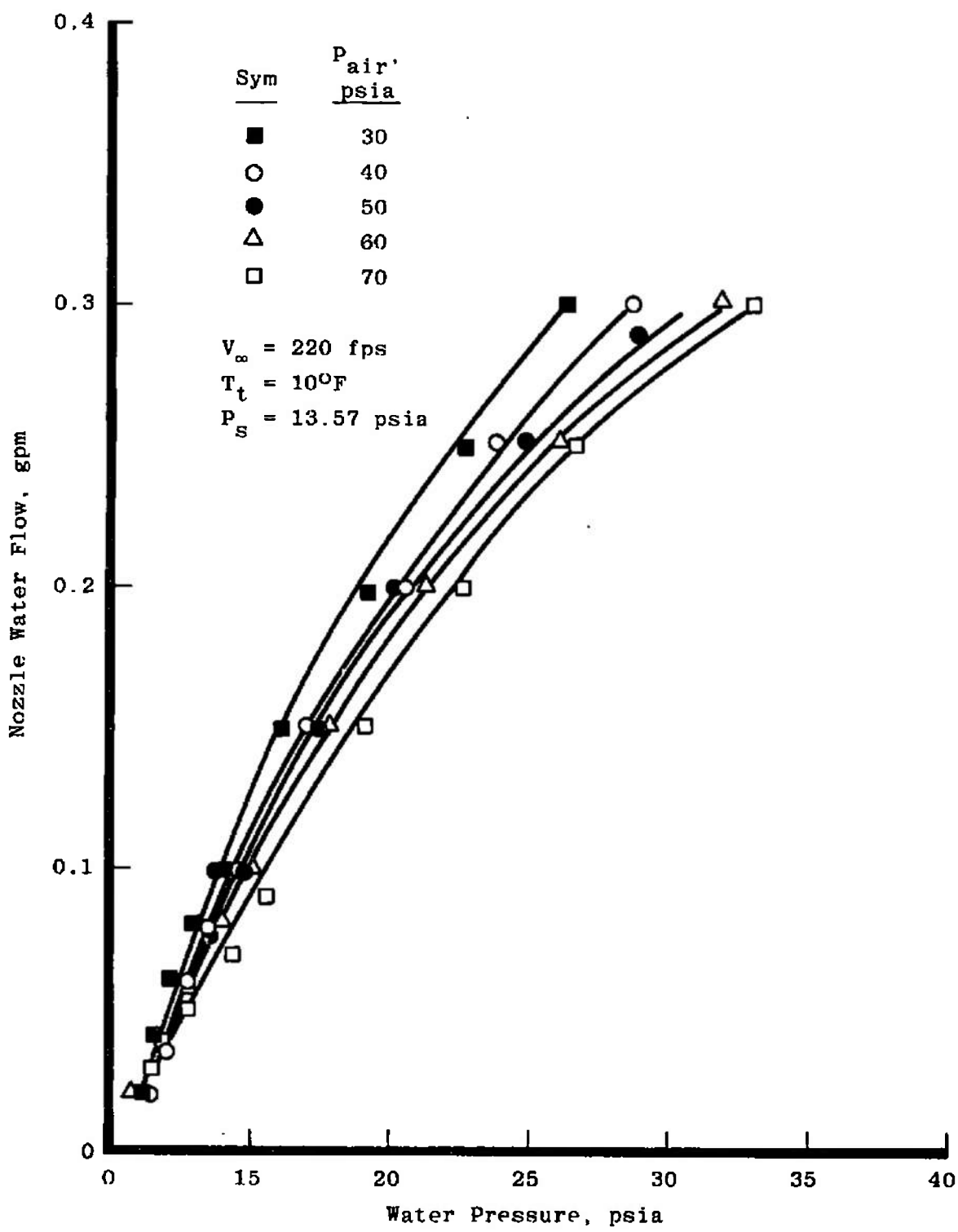


Figure 21. Water flow calibration, Sonicore #125 Nozzle.

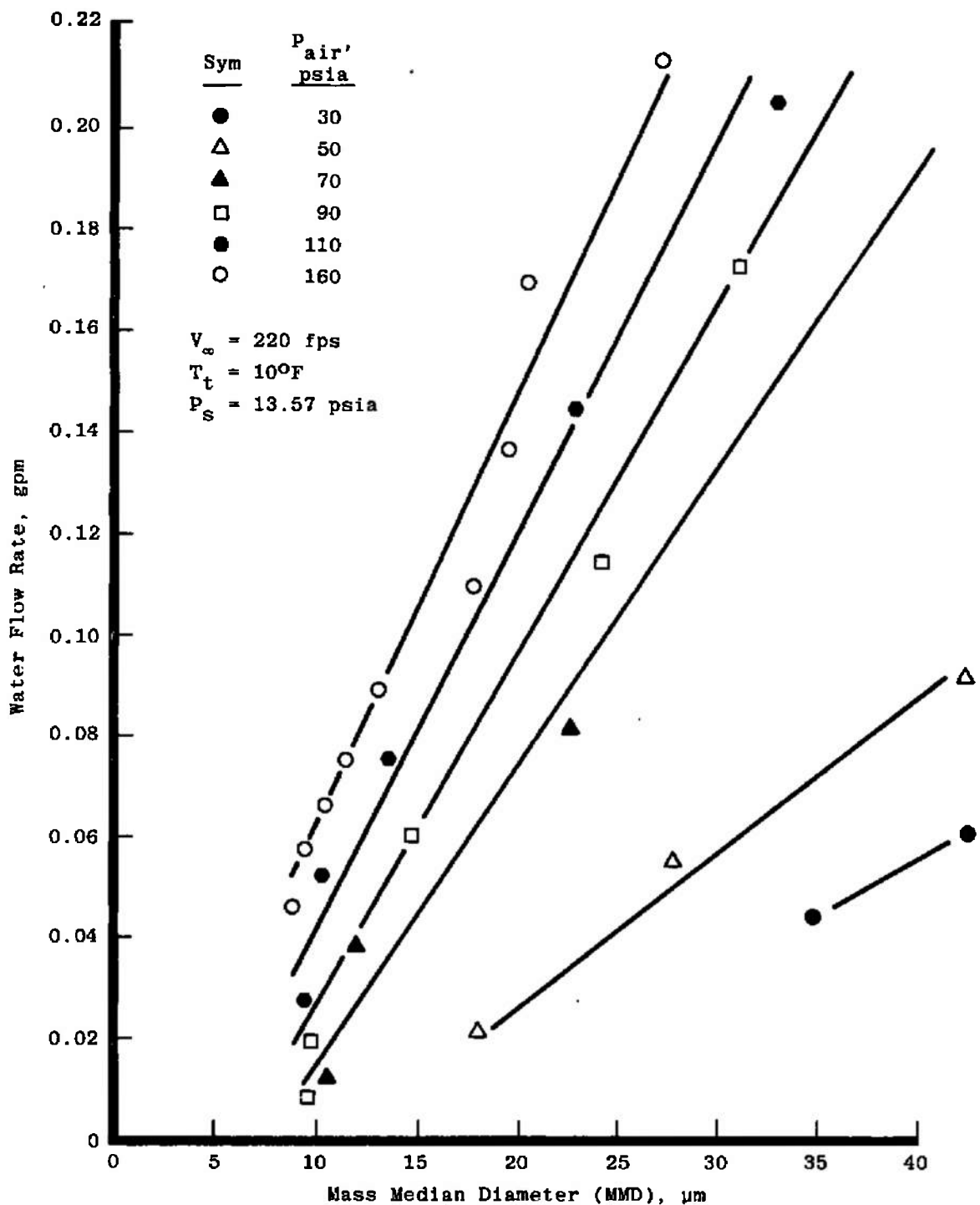


Figure 22. Droplet size calibration, Sonicore #052 Nozzle.

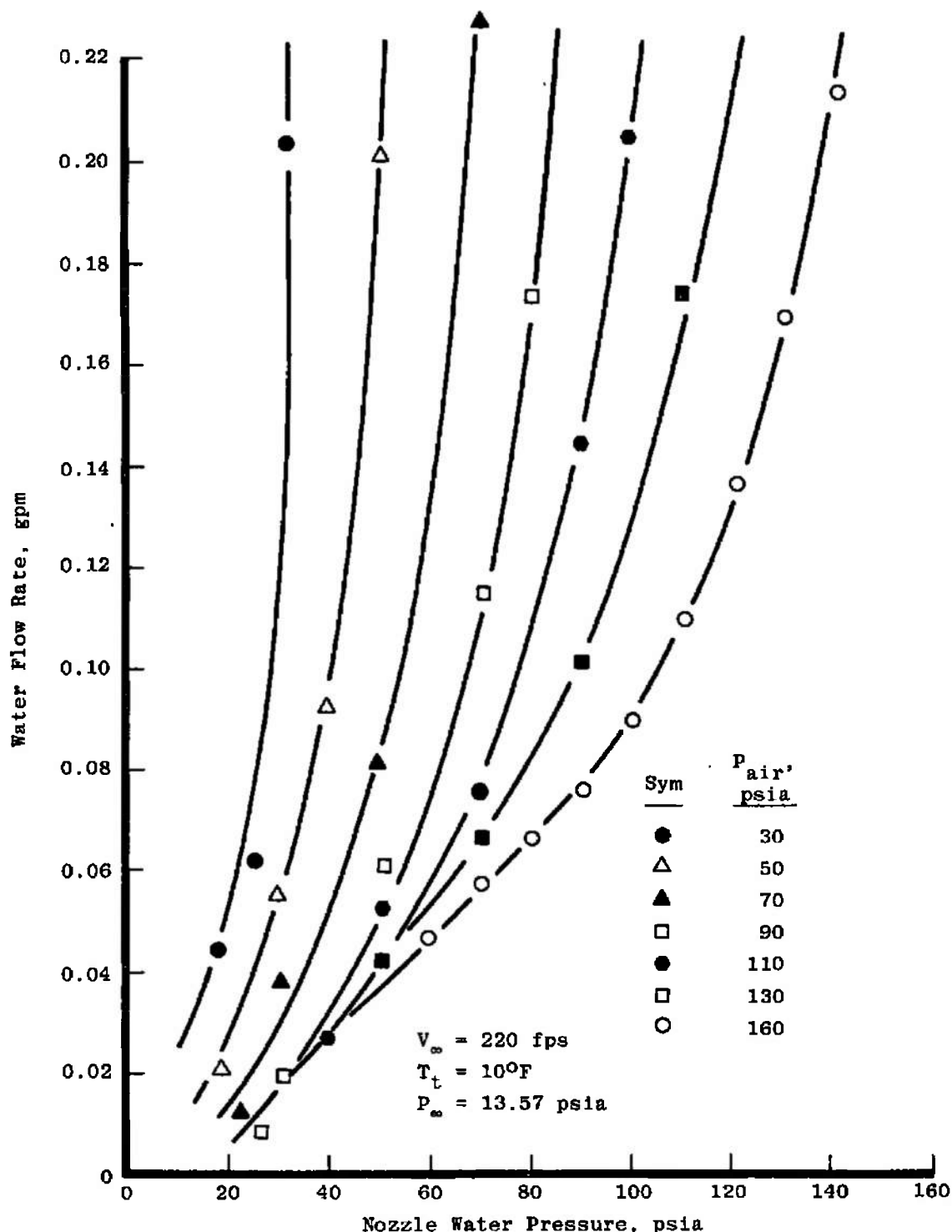


Figure 23. Water flow calibration, Sonicore #052 Nozzle.

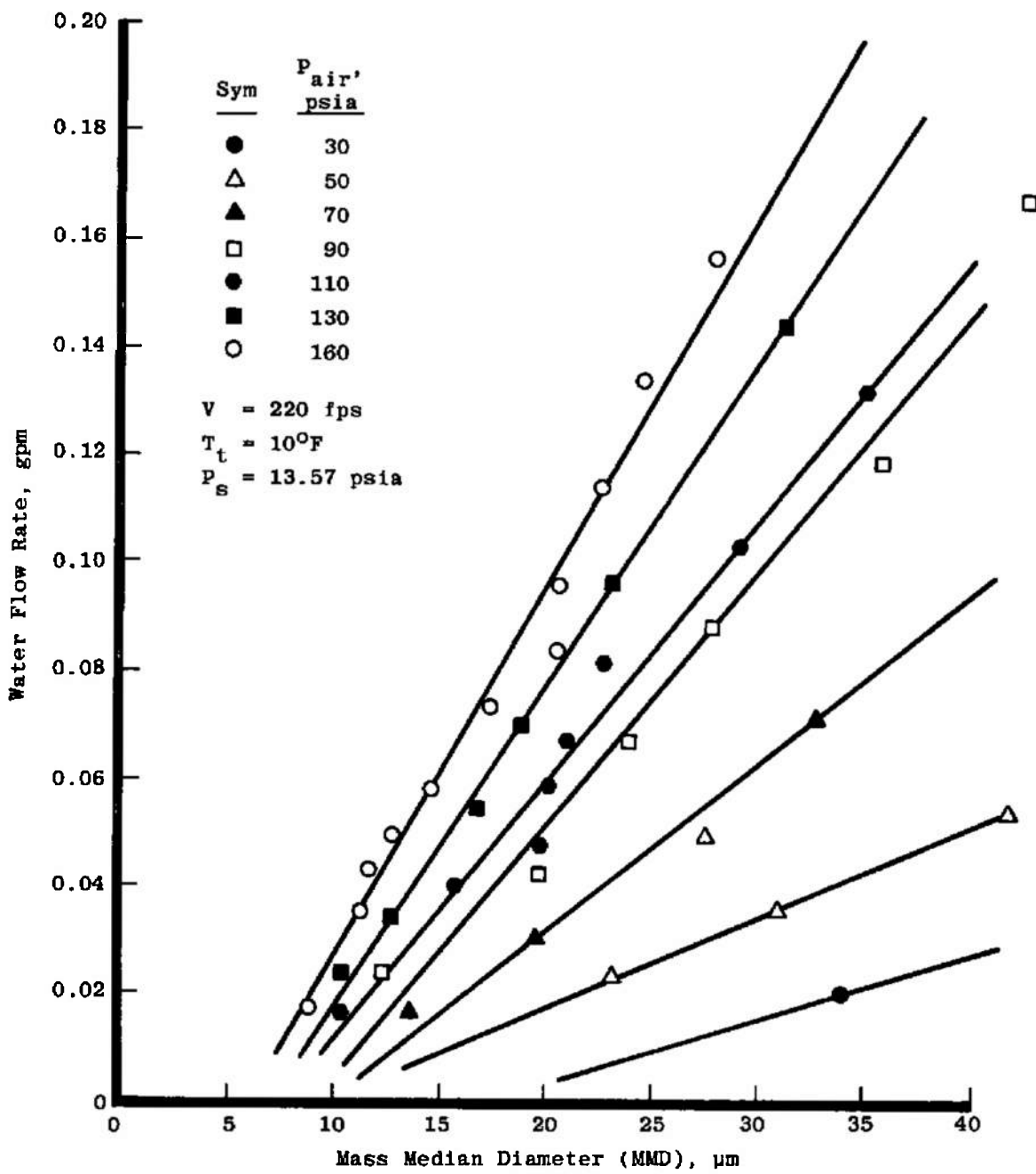


Figure 24. Droplet size calibration, Sonicore #035 Nozzle.

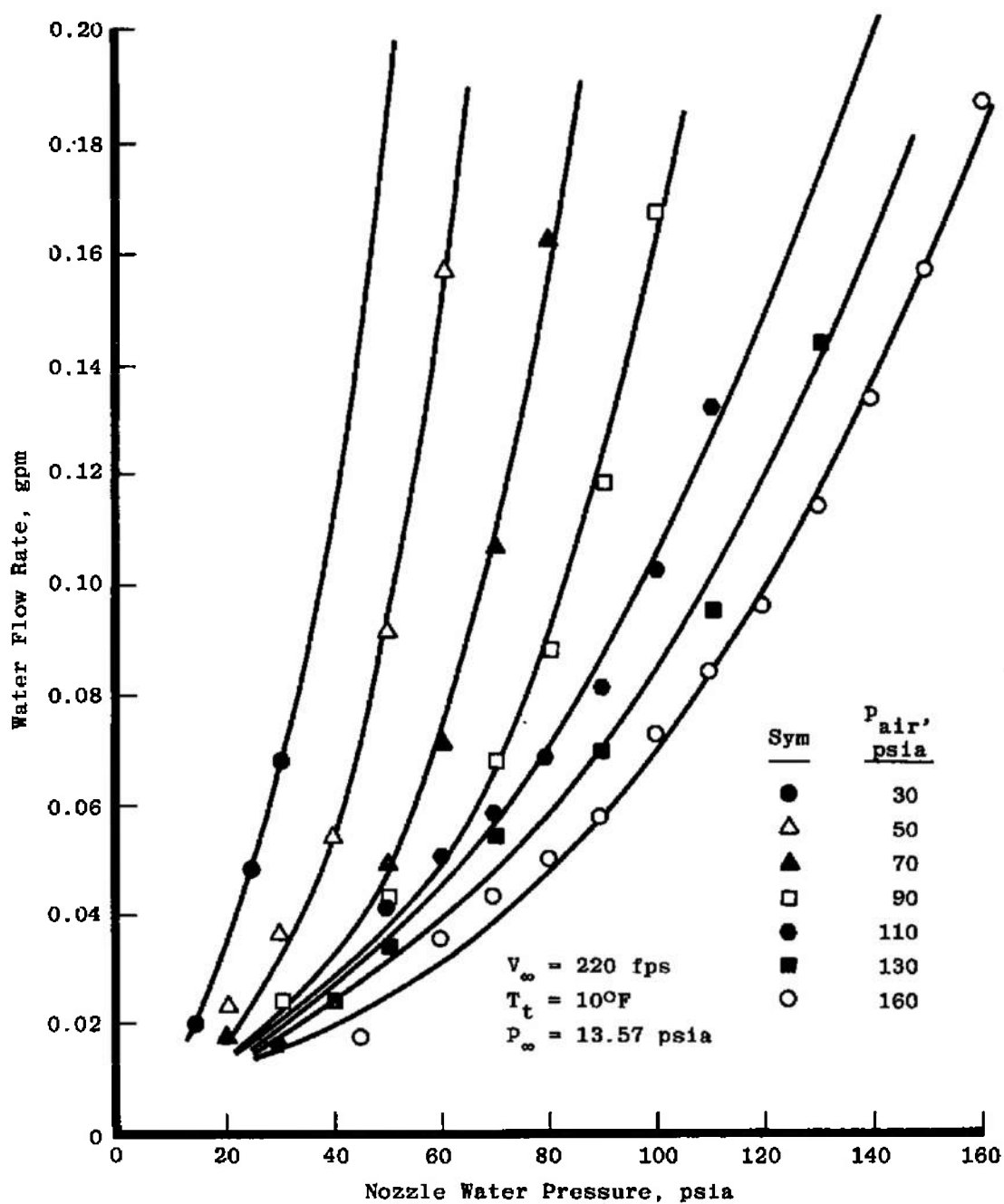
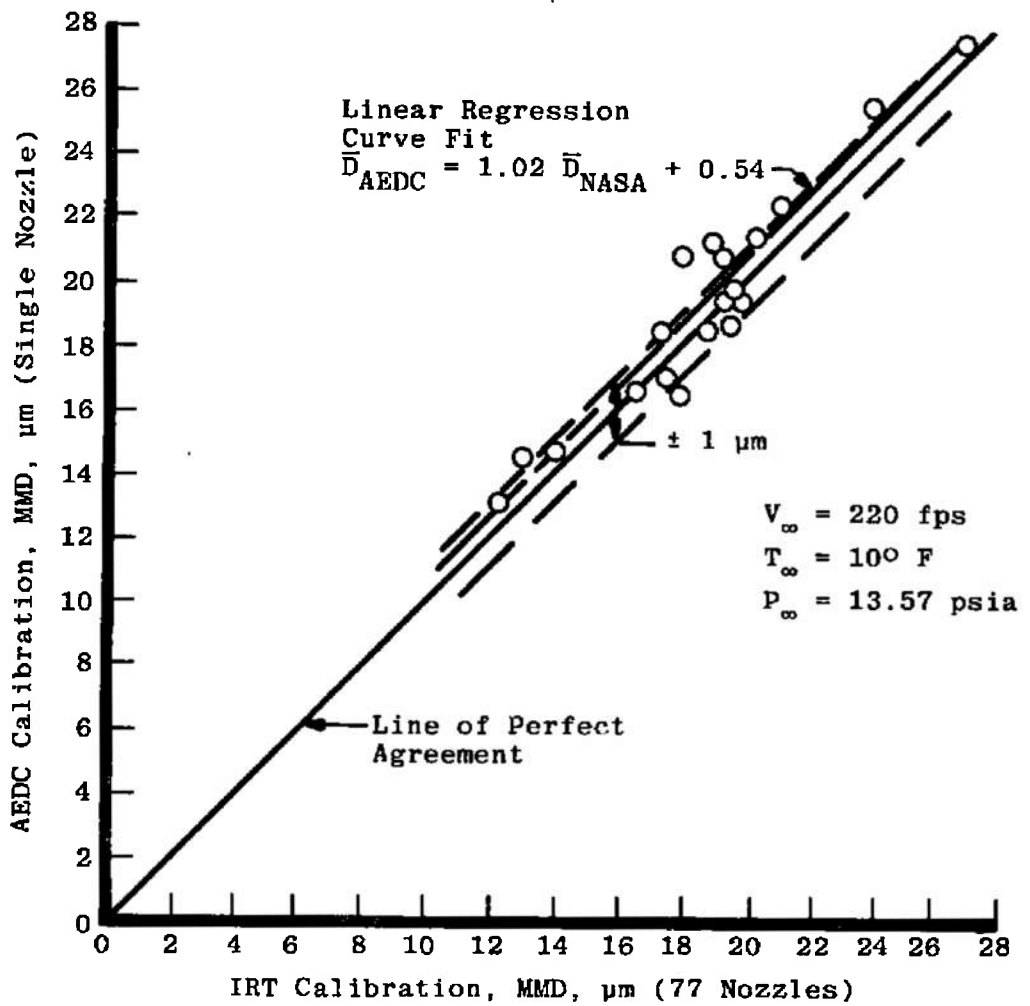


Figure 25. Water flow calibration, Sonicore #035 Nozzle.



**Figure 26. Scatter diagram AEDC versus NASA-LeRC calibrations of Standard NASA Nozzle.**

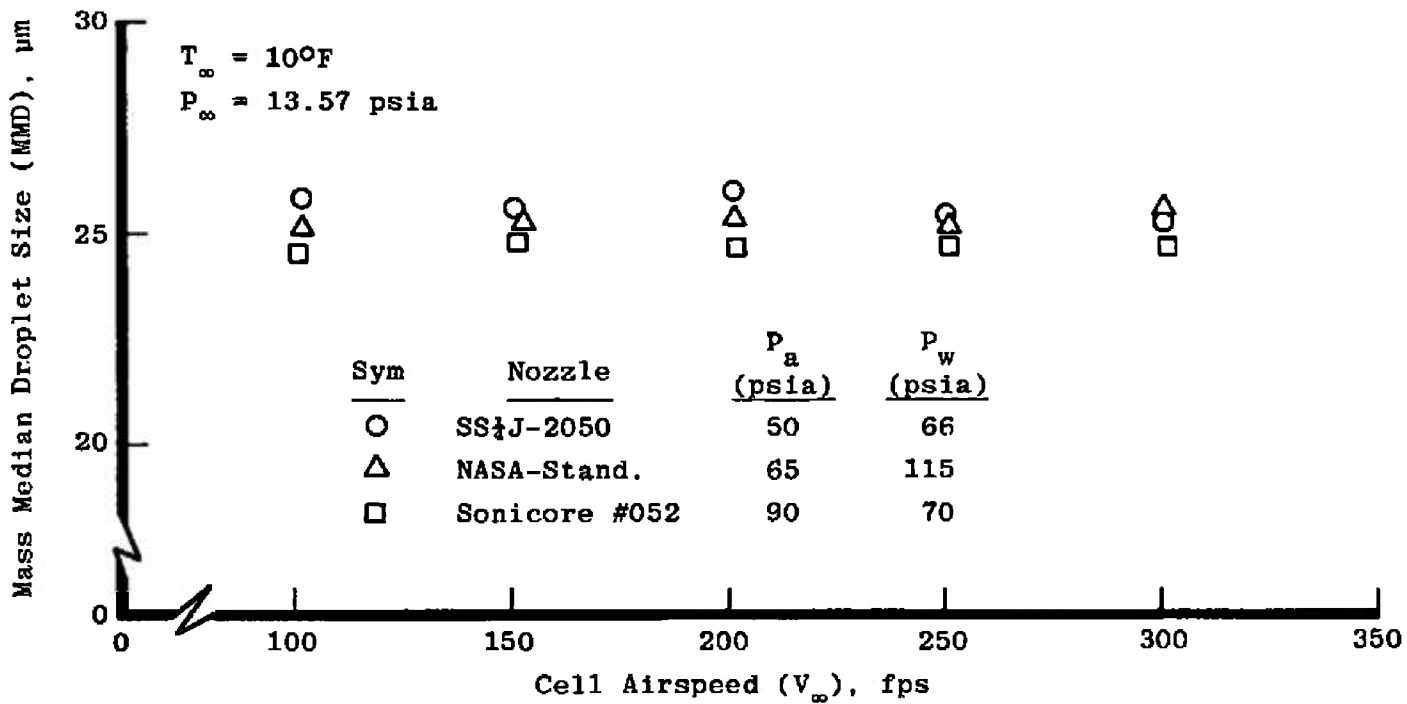


Figure 27. Effect of cell airspeed on calibration.

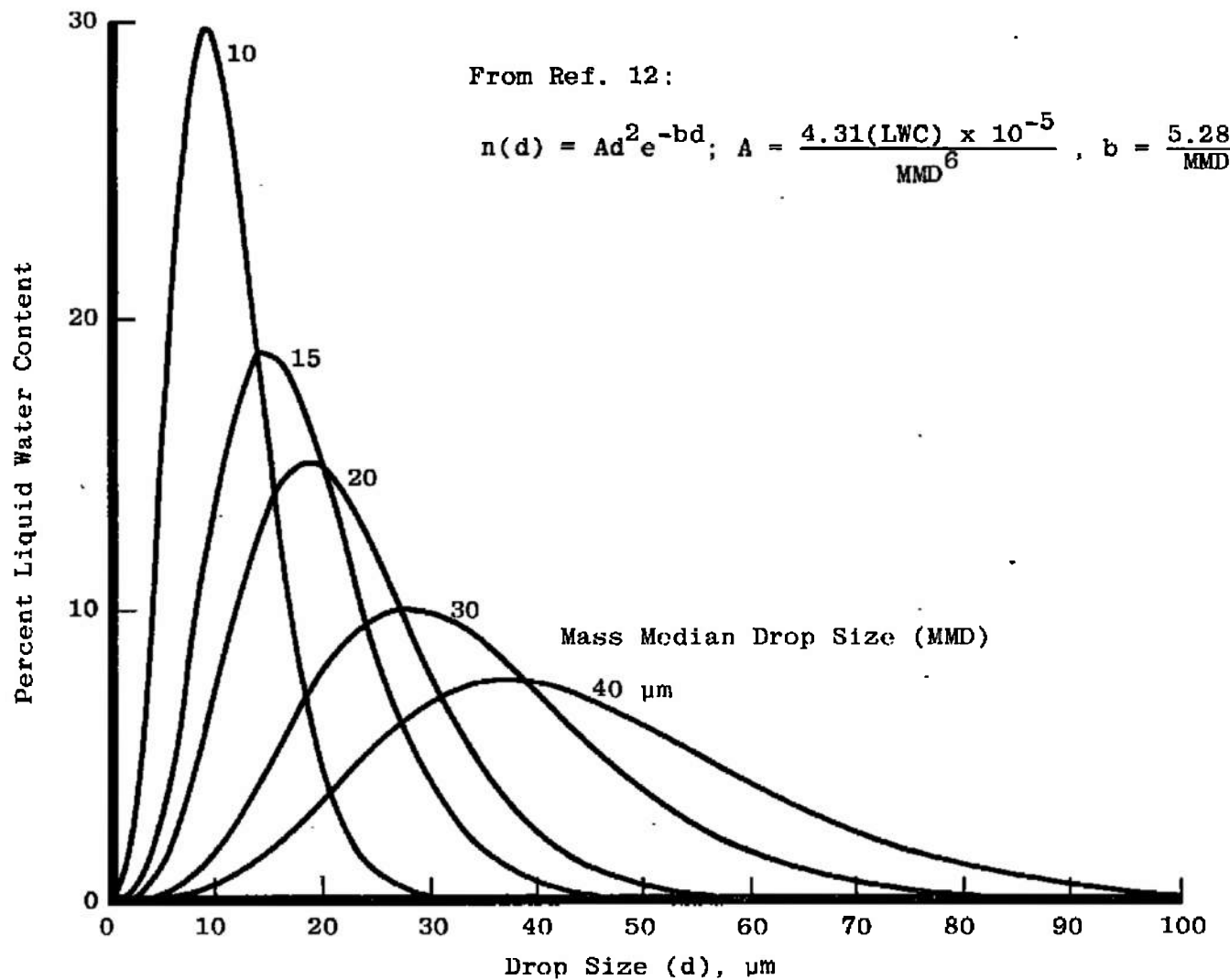


Figure 28. Drop size distribution in nature for a range of MMD at same LWC.

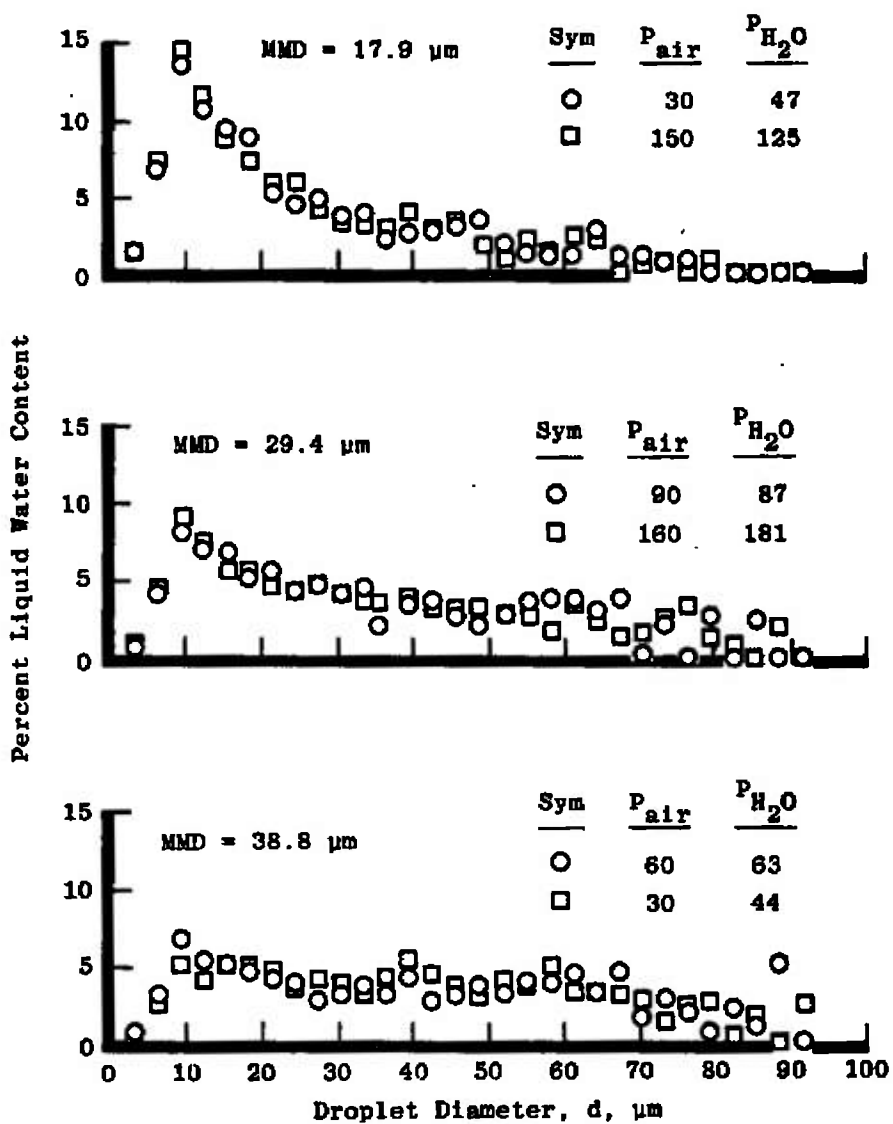
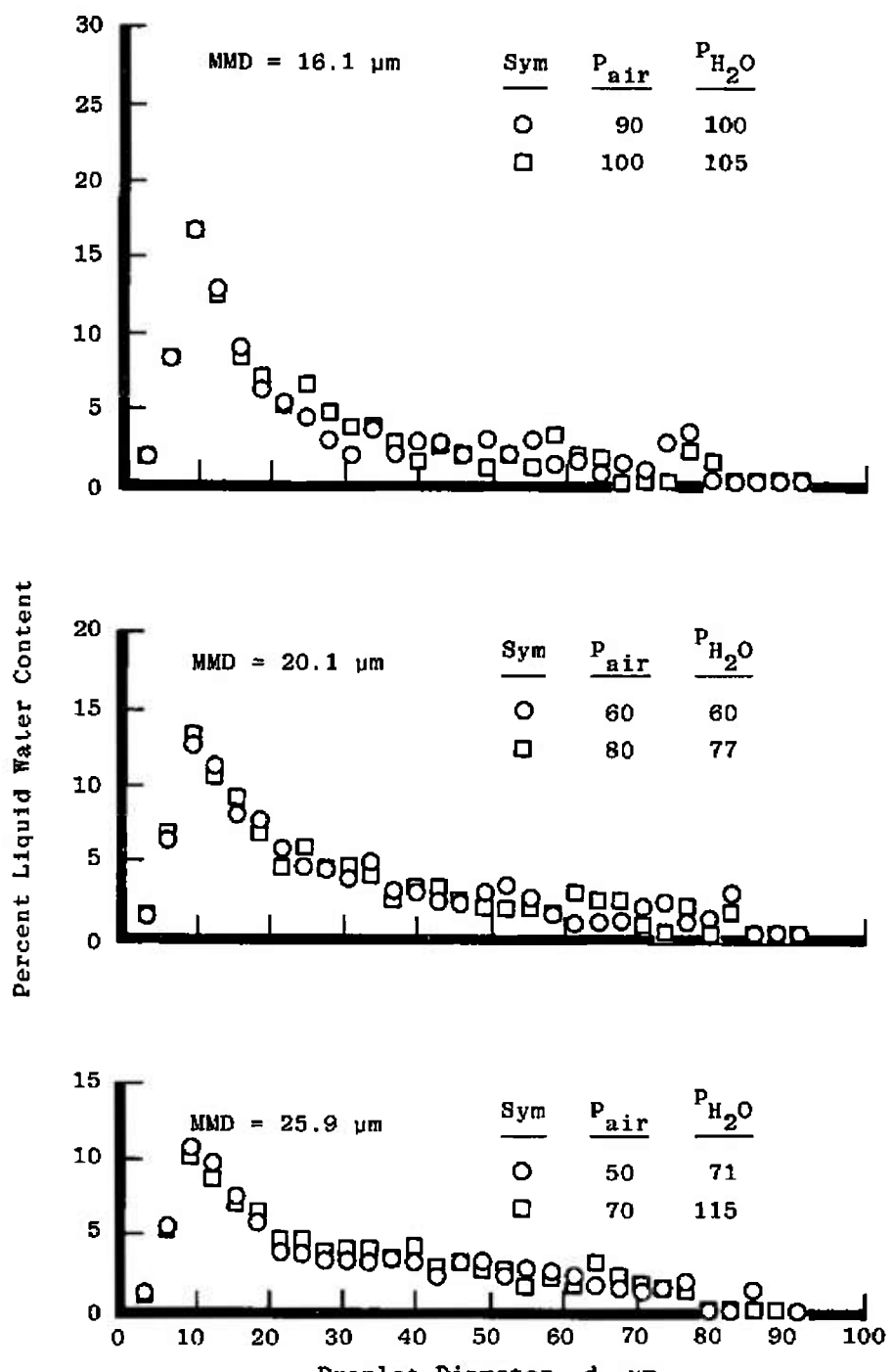
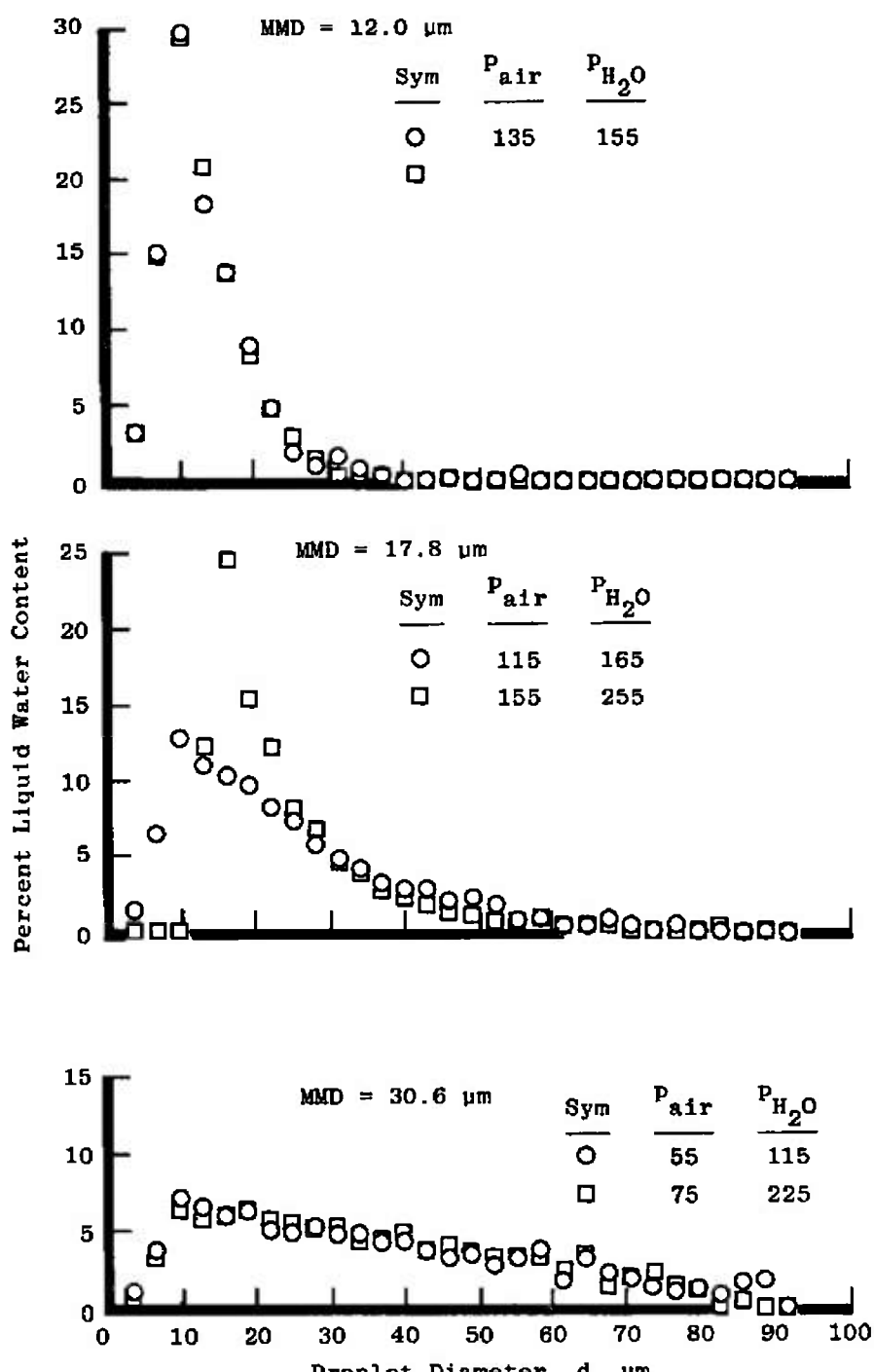


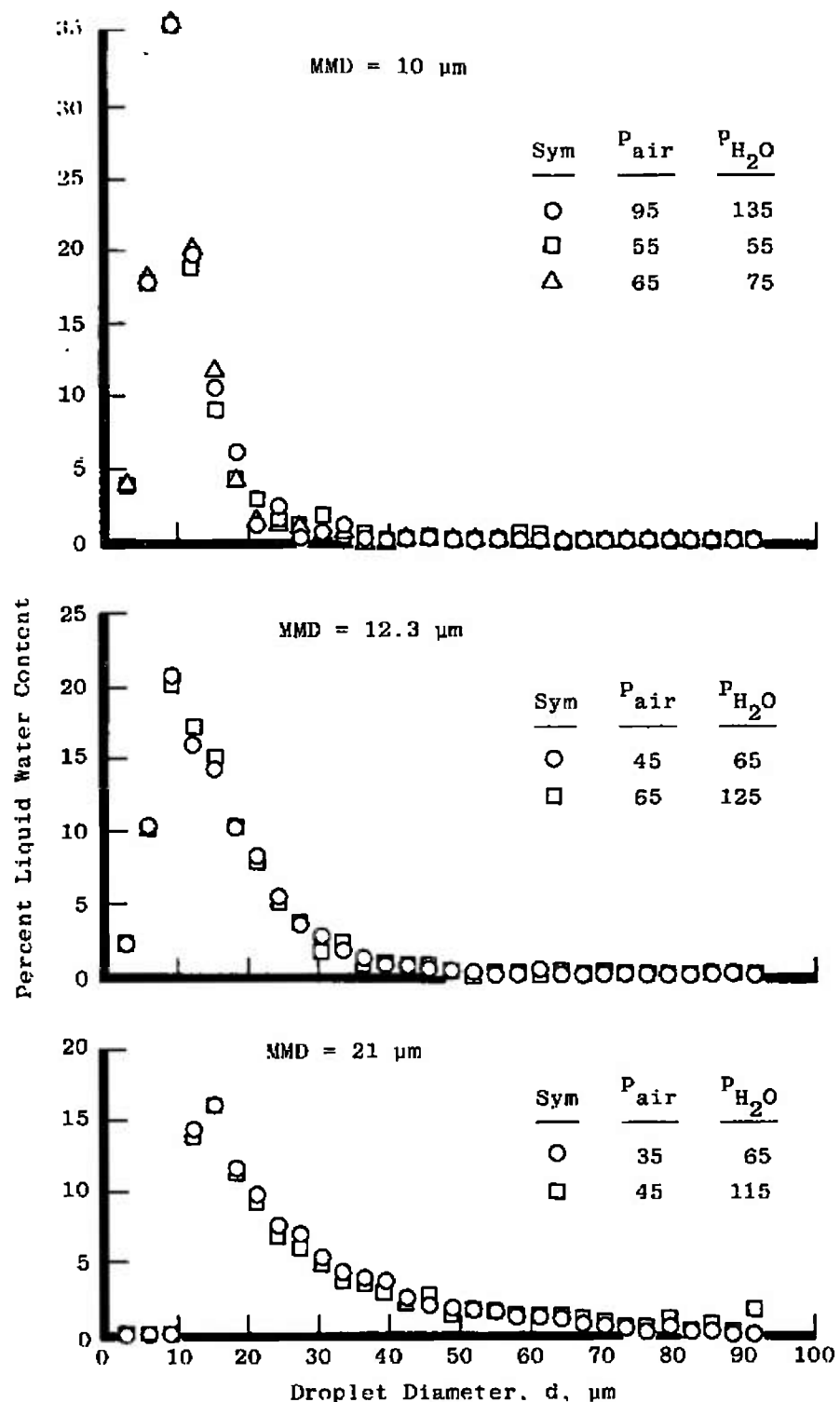
Figure 29. Droplet size distribution for nozzles.



b. SS $\frac{1}{4}$ J-2050  
Figure 29. Continued.

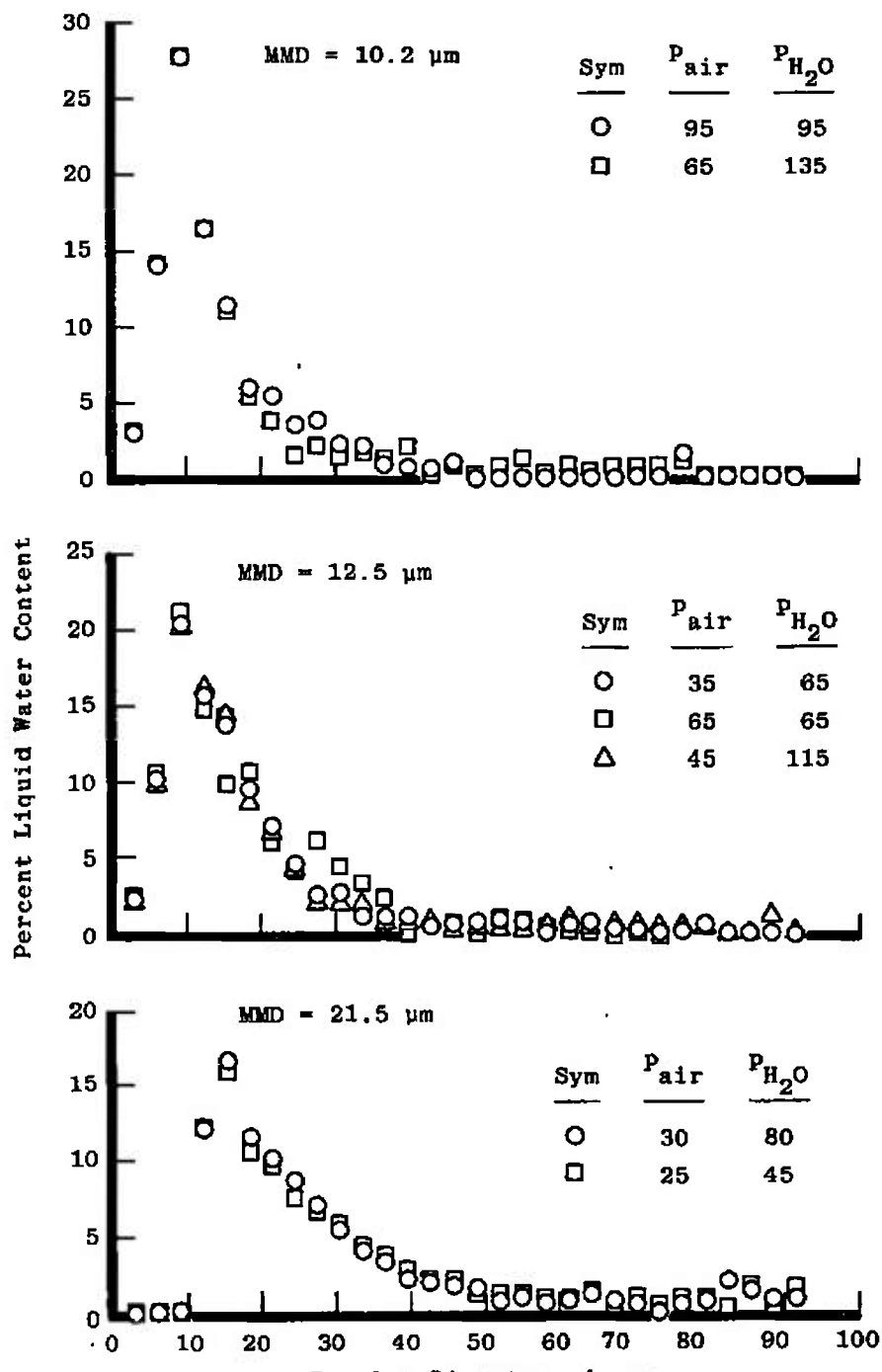


c. NASA-LeRC Standard  
Figure 29. Continued.



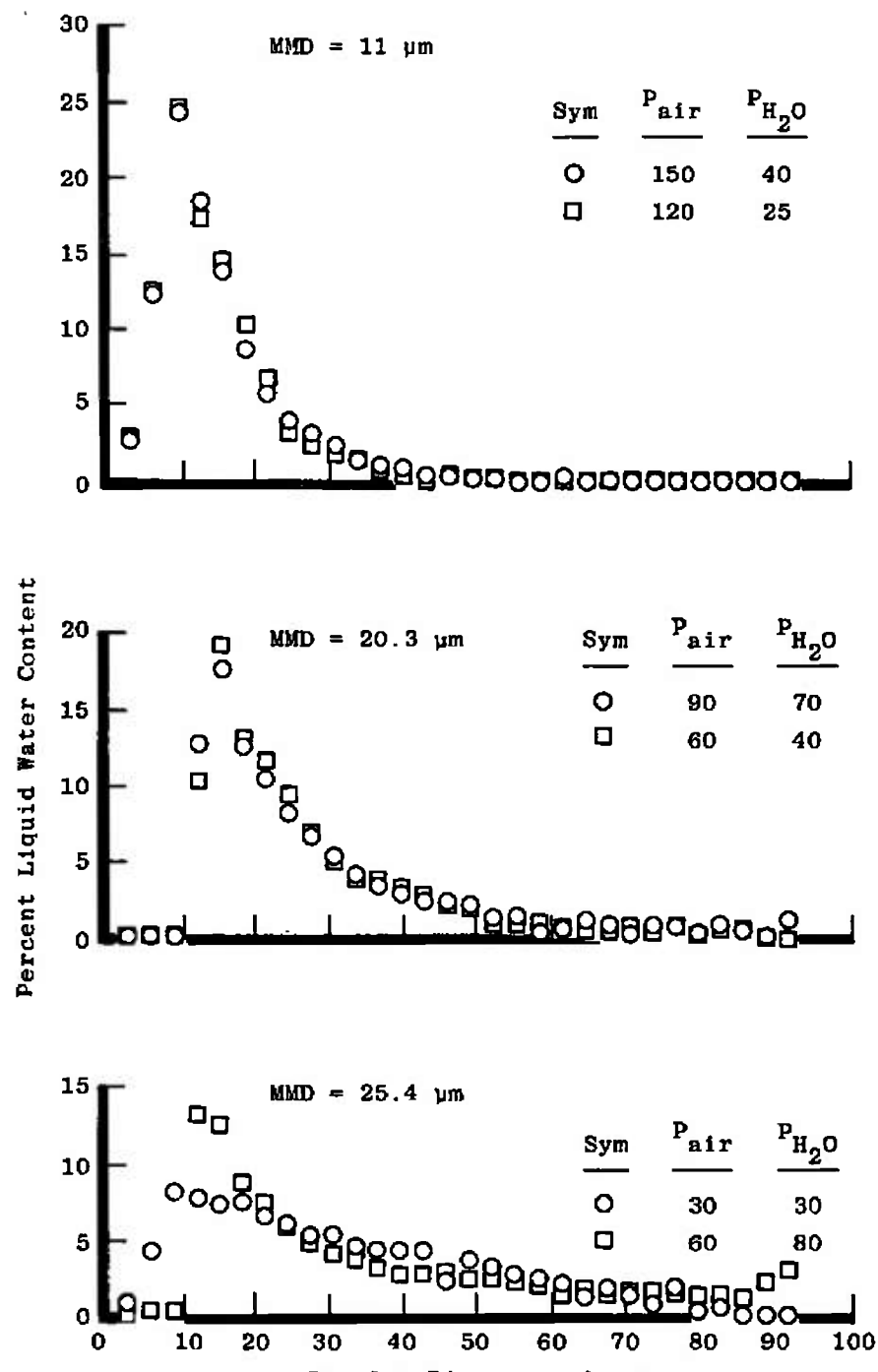
d. NASA-LeRC Model I

Figure 29. Continued.

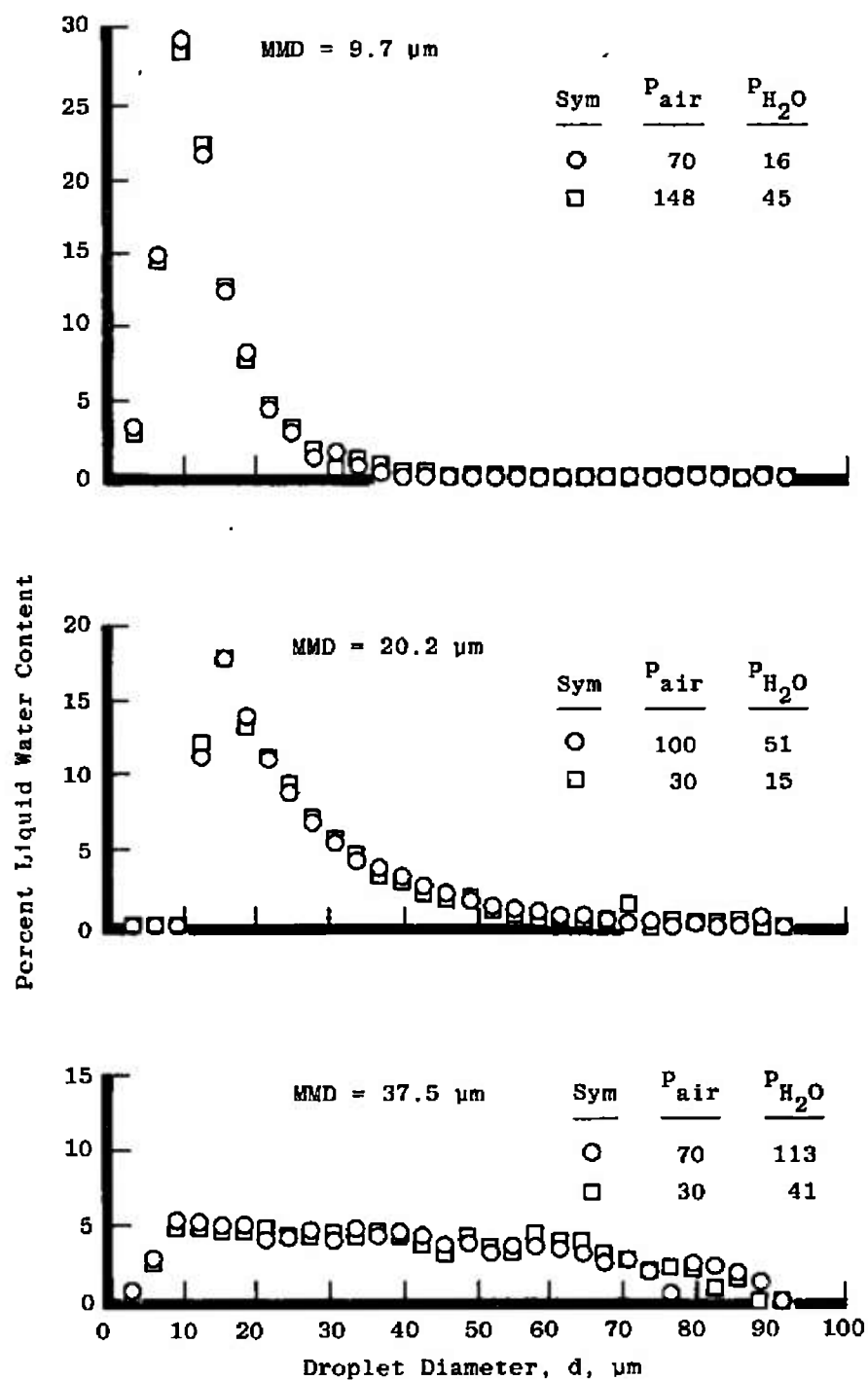


e. NASA-LeRC Model II

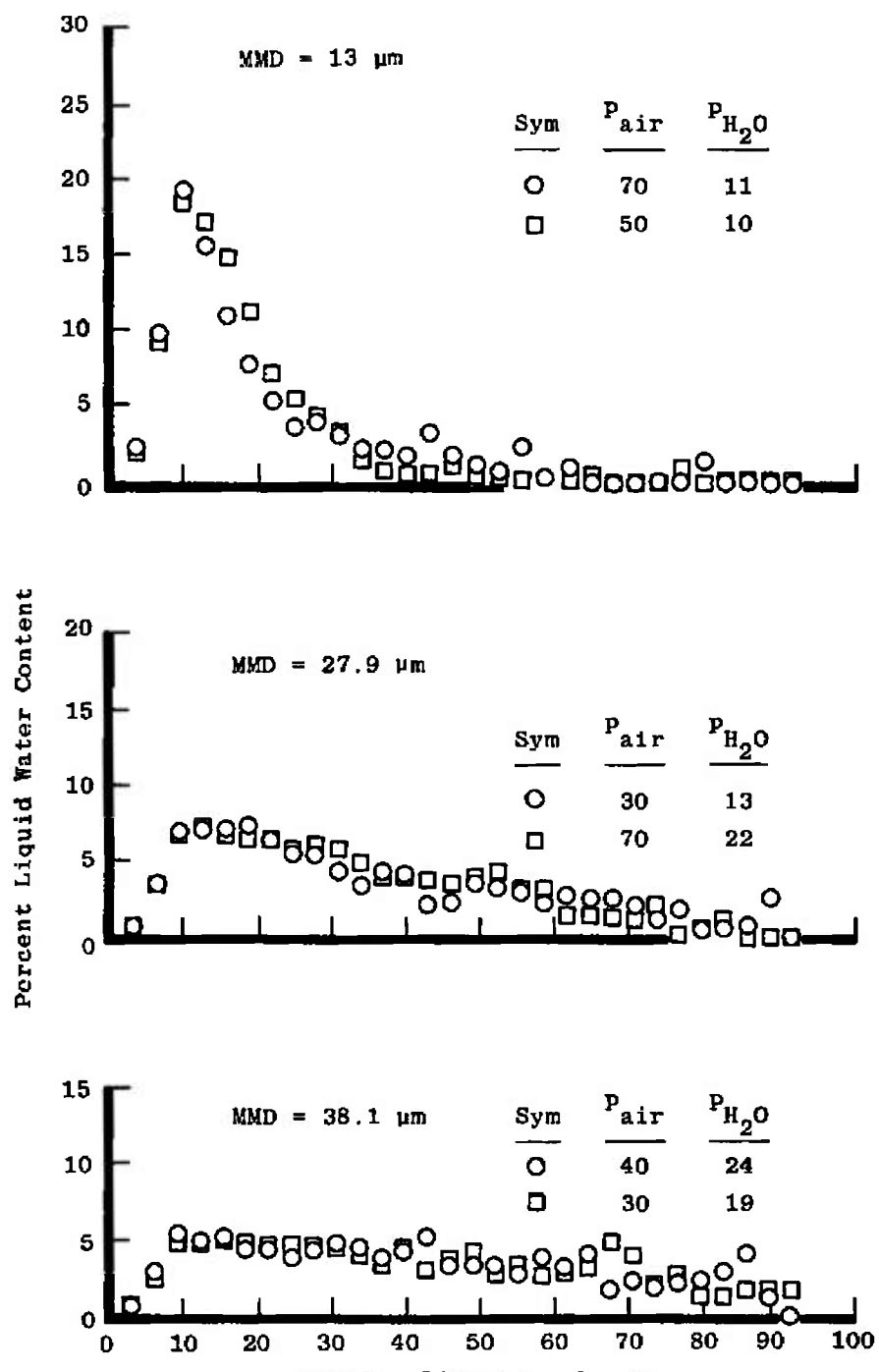
Figure 29. Continued.



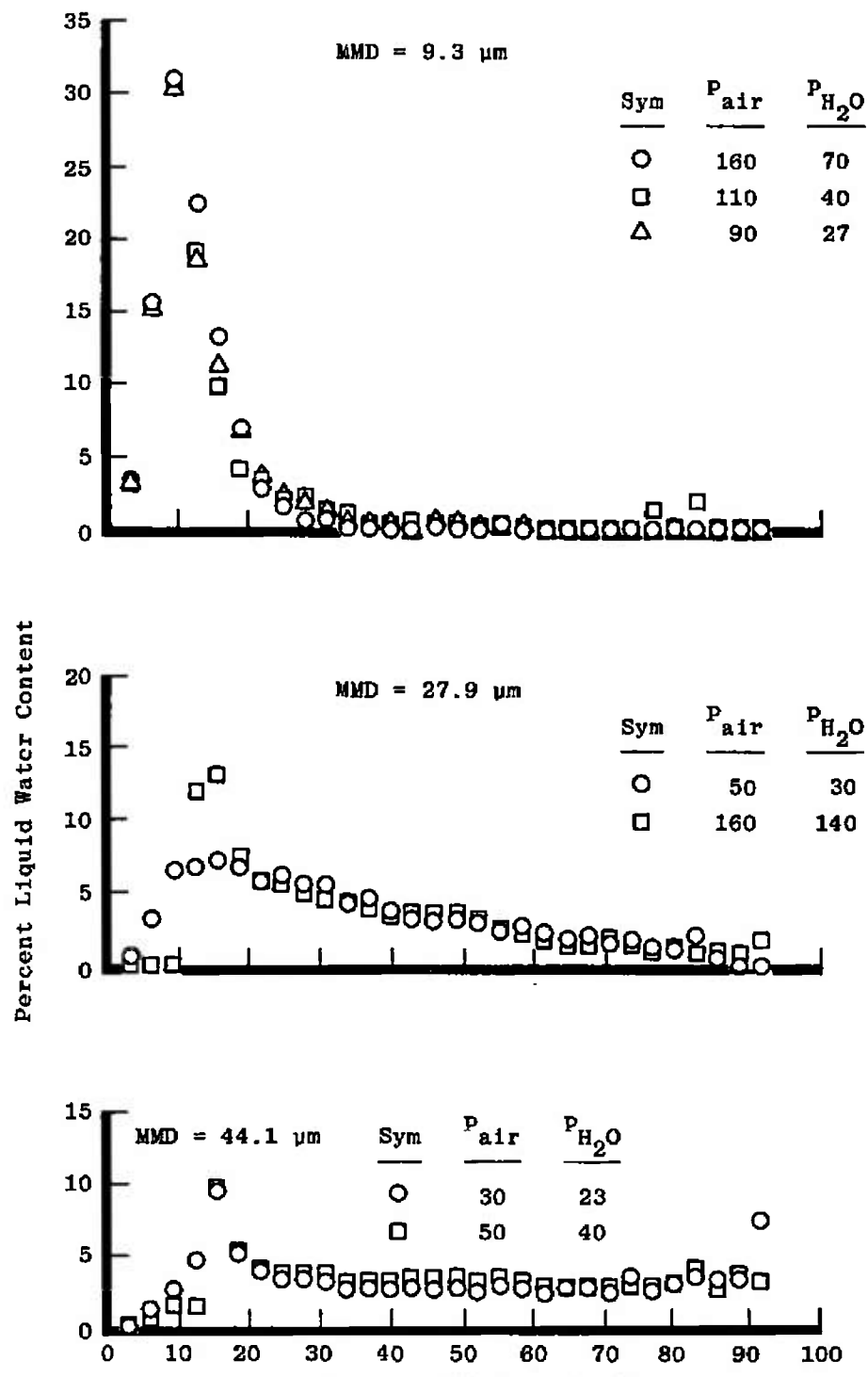
f. SS $\frac{1}{4}$ J-1A  
Figure 29. Continued.



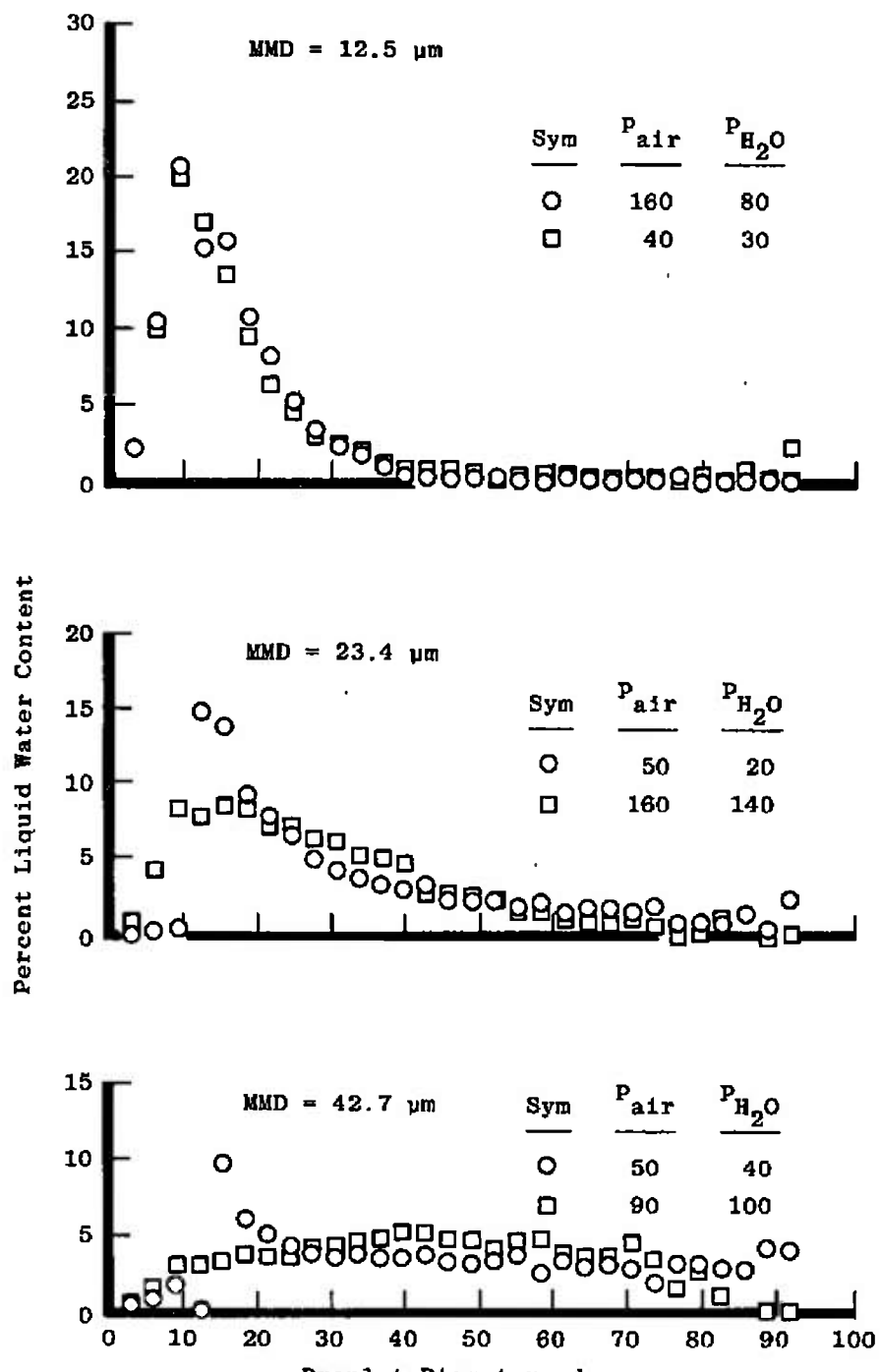
g. SS $\frac{1}{4}$ J-1  
Figure 29. Continued.



h. Sonicore #125  
Figure 29. Continued.



i. Sonicore #052  
Figure 29. Continued.



j. Sonicore #035  
Figure 29. Concluded.

**Table 1. Icing Research Cell Performance Capability**

Conditions	Level	
	Maximum	Minimum
Pressure Altitude	80,000 ft	Sea Level
Inlet Air Pressure	40 psi	---
Inlet Air Temperature	185°F	-20°F
Cell Mach Number	0.7	---
Airflow Rate	30 lbm/sec	---
Atomizing Air Pressure	175 psia	Atmospheric
Atomizing Air Temperature	200°F	70°F
Atomizing Air Flow Rate	15 SCFM	1.5 SCFM
Demineralized Water Temperature	200°F	Atmospheric
Demineralized Water Flow Rate	6 gph	0.6 gph

**Table 2. Parameter Measurement Uncertainty**

Parameter	Range	Bias (%) B	Precision Index (%), S	Degrees of Freedom	Uncertainty (%), $\pm(B + t_{95} S)$
Airflow	< 30 lbm/sec	0.12	0.17	> 30	0.45
Total Temperature	460°R	0.4	0.20	> 30	1.40
Total Pressure	5 to 30 psia	0.4	0.30	> 30	1.0
Water Flow	0.6 - 6 gph	0.1	0.14	> 30	0.3
Spray Nozzle Airflow	1.5 - 15 SCFM	2.23	1.00	> 30	5.46

**NOMENCLATURE**

<b>A</b>	Constant
<b>b</b>	$6/d_{avg}$ , $\mu\text{m}^{-1}$
<b>D<sub>AEDC</sub></b>	MMD from AEDC calibration, $\mu\text{m}$
<b><math>\bar{D}_m</math></b>	MMD, $\mu\text{m}$
<b>d</b>	Droplet diameter, $\mu\text{m}$
<b>d<sub>avg</sub></b>	Average droplet diameter, $\mu\text{m}$
<b>LWC</b>	Liquid water content, $\text{g}/\text{m}^3$
<b>MMD</b>	Mass median diameter, $\mu\text{m}$
<b>n(d)</b>	Droplet size distribution density, $\text{cm}^{-3}$
<b>P<sub>a</sub></b>	Atomizing air pressure, psia
<b>P<sub>∞</sub></b>	Free-stream static pressure, psia
<b>P<sub>w</sub></b>	Spray nozzle water pressure, psia
<b>T<sub>t</sub></b>	Total temperature, °F
<b>V<sub>∞</sub></b>	Free-stream velocity, ft/sec
<b>W<sub>a</sub></b>	Mass flow rate of spray nozzle atomizing air, lbm/sec
<b>W<sub>w</sub></b>	Mass flow rate of spray nozzle water, lbm/sec